Next 2 Page(s) In Document Denied

ELECTRICAL POTENTIAL VARIATION LAYERS NEAR ELECTRODES

G.A. Liubimov

Institute of Mechanics, Moscow State University, USSR

Certain problems of magnetic hydrodynamics have to deal with the flow of gas contacting the surface of a conductor. If the surfaces are the electrodes, with the flow confined between them, i.e., the surfaces through which there occurs exchange of current between the gas and an "external" object, the boundary condition is frequently specified as the current density on the surface of the electrode $/j_x/_s = f(xz)/$ or, which is the same, the potential difference between the two electrodes. Such boundary conditions presuppose that the current density on the interface specified or determined from the given potential difference is ensured by the mechanisms of the current transfer on the gas-electrode surface.

On the other hand, the current density on the surface of an electrode is determined, as we know, by the emission properties of the electrode material, its temperature and the intensity of the electric field near the electrode surface /1/. With small electric fields E on the electrode surface, the current density can be determined by the ration

$$J_{el} = AT^2 \exp\left[-\frac{e\Phi}{KT} + \frac{4.39}{T}\sqrt{E}\right] \qquad (1)$$

where Φ is the work function of the electrode material and T—its temperature.

The relationship /1/ shows that the current density on the surface of the electrode cannot, generally speaking, be specified or determined from the solution of the problem of current distribution in the gas. It has been shown in a number of editions, for example in /2, 3/, that when the boundary conditions are specified on the surface of the electrode, account should be taken of the possibility of formation of narrow layers of the electric potential change at the electrode. Such layers make the change in the potential in the flow area different from the potential difference on the electrodes. The

tial in the layer at the electrodes is determined from the condition of uninterrupted current density on the surface of the electrode and depends on the properties of the electrode material and the physical processes which occur near the surface of the electrode.

Since we know very little of the structure of the electrode layer, we must allow for certain assumptions, which can be specified more accurately or verified by comparison with the experimental data, to solve our problems.

As the simplest resort we may replace the electrode layers by the potential breaking surface /2/. For the next approximation we may assume that the potential has a linear distribution inside the layer, in which case

$$E = \frac{\varphi}{d} \qquad (2)$$

where d is the Debye length /3/.

From the assumption /2/ and the balance of the charged particles on the electrode surface we obtain the following ratio for determining the change in the potential in the electrode layer, depending on the current density

$$j = \frac{j_e \exp\left\{-\frac{e\varphi_\pm}{\kappa T}\right\} \pm (j_{el} + j_i)}{1 - \frac{1}{2}\left(1 - \Psi\left[\sqrt{\frac{2e\varphi_\pm}{\kappa T}}\right]\right)} \qquad (3)$$

where $j_e = n_e e\sqrt{\frac{\kappa T}{2m_e\pi}}$, $j_i = n_i e\sqrt{\frac{\kappa T}{2\pi m_i}}$, Ψ is the integral of probability.

If we regard the electrode layer as the breaking surface of the potential /2/ we shall obtain, instead of /3/, the following expressions

$$\varphi_+ = \frac{\kappa T}{e} \ln \frac{j_e}{j_i + j_{el} - j}, \quad \varphi_- = \frac{\kappa T}{e} \ln \frac{j_e}{j_i + j_{el} + j}. \qquad (4)$$

The volt-ampere characteristic for the gas interval, to which the potential difference V is applied, and with account taken of the layers at the electrodes, will have the following form /4/

$$V = jr + \varphi_+(j) - \varphi_-(j). \qquad (5)$$

The characteristic /5/ is actually nonlinear (if we disregard the layers at the electrodes, the characteristic will be linear: $v = rj$). Obviously, from the standpoint of their effect on the volt-ampere characteristic, the electrode layers can be described by certain resistance $r^0 = \frac{\varphi_+ - \varphi_-}{j}$ which depends on the current density.

The shape of the characteristic /5/ depends on the structure of the layer at the electrodes. If we use the assumptions in /4/ the characteristic has a saturation current area. With the assumptions in /3/ there is no current saturation area. The experimental data obtained in /2/ show that the characteristic has no current saturation area and, at large concentrations of the seeding, the characteristic has a large slope angle at greater currents.

The comparison of the experimental data with the data calculated in /5/ demonstrates that the assumptions in /3/ describe better the qualitative (and even quantitative) aspects of the phenomenon in question than the assumptions made in /4/. In this connection, the theory based on the assumptions /2/-/3/ appears to be in good agreement with the experimental data when the temperature of the electrodes is $T \gtrsim 2000^\circ$.

References

1. V.I.Gaponov. "Electronics", Fizmatgiz, 1960.
2. Z.Croitoru, A.Montardy. "Electrode Phenomena, Tensor Conductivity and Electrode Heating in Seeded Argon." IV Symp. Eng. asp. magnetohydrodyn., 1963.
3. G.A.Lyubimov. "Change in the Electric Potential at the Channel Wall with an Ionised Gas Flowing in a Magnetic Field". Applied Mechanics and Technical Physics, 1963, No. 5.
4. G.A.Lyubimov. Electrode Layers of the Potential Change in Passing Weak Current Through an Ionised Gas, Applied Mechanics and Technical Physics, 1963, No. 6.

FORMATION OF SPACE CHARGE SHEATHS AND FLOW OF AN ELECTRIC CURRENT IN A PLASMA STREAM

INVESTIGATIONS OF IONIZATION CHARACTERISTICS OF PLASMA STREAMS IN AN ELECTRIC FIELD

A.K. Musin

V.I. Lenin All-Union Electrical Institute, Moscow, USSR

1. A theory developed by Thompson and Wilson [1,2] for a non-self-sustained current in a gap is often used for studies of ionization properties of plasmas. However, this theory is based on the assumption that processes associated with electric current flow are stationary. It is inapplicable to rapidly moving plasmas, plasmoids and flames. In this paper approximate analysis of setting up processes of non-self-sustained current and sheaths adjacent to the electrodes are given and basic setting up periods are defined. Thompson-Wilson's theory describing a steady non-self-sustained current may be regarded as a particular case when $t \to \infty$ (see also [3]).

2. Let a uniform ionized gas stream flows with steady velocity $\vec{V}$ into a space between two plane electrodes to which a constant external voltage U_o is applied [see fig. 1]. During this process the total electric current in external circuit remains constant. However, the current density will vary along the direction of the plasma flow because space charge sheaths and potential drops at the electrodes do not set up instantaneously. In a coordinate system associated with the flow certain expressions appears to be dependant on "equivalent" time $t = Z/V$. Equations of continuity and of field source in moving coordinate system may be written as follow ;

$$\frac{\partial n_i}{\partial t} + b_i \frac{\partial}{\partial x}(n_i E) = I - \alpha_r n_e^r n_i \; ; \qquad (1)$$

$$\frac{\partial n_e}{\partial t} - b_e \frac{\partial}{\partial x}(n_e E) = I - \alpha_r n_e^r n_i \; ; \qquad (2)$$

$$\frac{\partial E}{\partial x} = 4\pi e_o (n_i - n_e) \qquad (3)$$

Where n_i, b_i, n_e, b_e -are concentrations and mobilties of electrons and ions; E- is the electric field strength; I- the ionization rate; α_r- the effective recombination coefficient; $r \in (1,2)$- depending on a dominant recombination process. If it is assumed that the cathode and anode do not

tion equilibrium occurs when no electric field is applied, then the boundary conditions can be assumed to be:

$$n_i\big|_{x=x_0} = n_e\big|_{x=0} = 0\,; \quad \int_0^{x_0} E(x)\,dx = u_0\,; \tag{4}$$

$$n_i\big|_{t=0} = n_e\big|_{t=0} = n_0 = \left(\frac{I}{\alpha}\right)^{\frac{1}{(r+1)}}; \quad E\big|_{t=0} = E_0 = \frac{u_0}{x_0}\,. \tag{5}$$

Solution of the expressions (1)-(5) has been found in the form of continuous functions which are plotted in fig.2-4.

3. After the application of an external voltage the electrons move from the cathode and form a high current at the anode. A positive charge sheath forms near the cathode. As a result, an electric field at the cathode increases and causes considerable increase of the ion current. Simultaneously the thickness of the cathode sheath increases while electric field in a plasma gap decreases. This leads to a decrease of the electronic current to the anode. Soon the positive ion concentration near the cathode begins to decrease due to the difference in drift velocities of the ions in the cathode region and in the plasma gap. The ion current value, having approached the electronic current value and having passed maximum , decreases together with that of electronic current. When $t \to \infty$ all the values approach their limits asymptotically. Expressions for these limiting values coincide with formulas of the Thompson-Wilson's theory for a steady process. Principal form of the solution is given in fig. 4 and 5.

Electric field in the plasma gap /outside the space charge sheaths, fig. 4/ is given by the expression:

$$\left.\begin{aligned} E^{\lambda}(t) = E^{\lambda}_{\infty} &= \exp\left[\ln\frac{E_0}{E^{\lambda}_{\infty}}\exp\left(-\frac{t}{\tau_E}\right)^2\right]; \\ \tau_E &= \left[\frac{8(S+1)^3 n_0 b_e}{\pi e_0 I^3 b_i (b_i + b_e)}\right]^{1/4}; \\ E^{\lambda}_{\infty} &= \frac{1}{n_0}\left\{\left[\frac{I}{b_e(S+1)}\right]^3 \frac{2 b_i u_0^2}{\pi e_0 (b_i + b_e)}\right\}^{1/4} \end{aligned}\right\} \tag{6}$$

4. Setting up processes for the electric current and space charge sheaths may be divided into three periods:

4.1. Initial period $\left(t << \tau_E \ln^{-1/2}\left(\frac{E_0}{E^{\lambda}_{\infty}}\right)\right)$ during which the electric field in plasma gap changes insignificantly and a proportionality between the electric current and the external voltage is approximately maintained. Then the current-voltage characteristic takes the form

$$J \approx \frac{1}{3} \gamma_0 Z_0 \frac{U_0}{X_0} (2 e_0 b_e n_0 + \gamma) \qquad (7)$$

Wherefrom the plasma conductivity γ may be determined

4.2. Intermediate period $\left(\tau_{jk} >> t >> \tau_E \ln^{-1/2}\left(\frac{E_0}{E^{\lambda}_{\infty}}\right)\right)$ when $E^{\lambda}(t) \gtrsim E^{\lambda}_{\infty}$ and the ion concentration near cathode is $n_i^0 << n_0$. Pressures and ionization velocities being sufficiently high $\left(b_i \approx 1 \frac{sm/sec}{v/sm}, \; n_0 \gtrsim 10^{12} sm^{-3}\right)$ the current-voltage characteristic has the form $\left(\tau_{j1} = \left[\frac{(s+1)\pi}{2 e_0 b_i I (1+b_i/b_e)}\right]\right)$:

$$J \approx \gamma_0 e_0 n_0 \left(Z_0 V \frac{b_i}{\pi} U_0\right)^{1/2} \qquad (8)$$

Wherefrom the concentration of charged particles n_0 in the plasma may be determined.

In the opposite case of low pressures and small electron concentrations $\left(b_i \approx 10 \frac{sm/sec}{v/sm}, \; n_0 \lesssim 10^{12} sm^{-3}\right)$ the current-voltage characteristic has the form $\left(\tau_{j2} = \frac{n_0 (s+1)}{I (1+b_i/b_e)}\right)$:

$$J \approx \frac{1}{2} \gamma_0 \left[\frac{2 b_i Z_0 U_0^2}{\pi (1+b_i/b_e)} (V e_0 n_0)^3\right]^{1/4} \qquad (9)$$

Wherefrom the concentration of the charged particles n_0 may be determined too.

4.3. Steady current period $\left(\tau_{jk} << t \to \infty\right)$ is characterized by the constancy of the electrode current density. The current-voltage characteristic then has the form

$$J = \gamma_0 Z_0 \left\{\left[\frac{e_0 I (1+\frac{b_i}{b_e})}{(s+1)}\right]^{(3)} \frac{2 b_i U_0^2}{\pi}\right\}^{1/4} \qquad (10)$$

and does not depend directly on concentration of the charged particles but allows to find the ionization rate I in the

5. Application of the described theory to the results of Boucher's [4] (fig.6) and Banta's [5] (fig.7) experiments are given below as an illustration. These authors have investigated ionization properties of air flames at combustion temperature $T \sim 2 \cdot 10^3\,^\circ K$ (natural gas - air mixture) with additives NaCl [4] and KCl [5]. Experimental points of current-voltage characteristics are denoted by circles with crosses. Electron concentrations n_e were determined from formula (9): continuous straight line denotes the mean value of $\bar{n}_e$, squares correspond to experimental points of the current-voltage characteristic. Corresponding temperature $T_e = (2,1 \pm 0,1) \cdot 10^3\,^\circ K$ is in good agreement with measured temperature ($T \sim 2 \cdot 10^3\,^\circ K$)

Circles with points denote measured values for thickness λ of cathode positive charge sheath in the center of an electrode.

Positive ion mobility may be found from formula

$$b_{i1} = \pi \frac{j \lambda^3}{U_{01}^2} \qquad (11)$$

Dashed lines denote mean values of $\bar{b}_i$, squares correspond to experimental points of the current-voltage characteristic. The upper dashed line (b_{ist}) was obtained when the current was assumed to be steady (Thompson-Wilson's theory). Density of the electrode current was assumed to be constant and equal J/S . Lower dashed line (b_{inst}) was obtained accounting current density variations along the electrodes. It is to be noted, that in fig.7 both dashed lines are located close to one another and practically coincide (within the limits of experimental errors), while the values $\bar{b}_{ist}$ and $\bar{b}_{inst}$ in fig. 6 differ significantly (more than twice). This may be explained by the fact that [illegible] with guard rings over

which current density was practically constant, and from formula $j = J/S$ the author has obtained the current density value close its true value. Boucher [4] (fig.6), on the contrary, has used electrodes without guard rings and using the formula $j = J/S$ he obtained excessive (2,38 times) value of current density in the centre of electrode. Values of ion mobilities calculated with an account of the current density variations, satisfy the Langevin's relation well

$$\frac{b_{i1}}{b_{i2}} = \frac{1 + (M_{i1}/M_g)}{1 + (M_{i2}/M_g)} \qquad (12)$$

where M_g -is mass of initial gas molecule: in our case

$$\frac{b_{iNa}}{b_{iK}} = \frac{7,2}{6,9} \approx 1,05$$

while the formula (12) gives the value equal to 1,09.

It is also to be noted that values $b_{iNa} = (7,2 \pm 0,5) \frac{sm/sec}{v/sm}$ and $b_{iK} = (6,9 \pm 0,5) \frac{sm/sec}{v/sm}$ are close to the values $b_{iNa} \approx 7,9 \frac{sm/sec}{v/sm}$ and $b_{iK} \approx 7,3 \frac{sm/sec}{v/sm}$ which are obtained from Brown's data [6] ($b_{iNa} \approx 2,97 \frac{sm/sec}{v/sm}$, $b_{iK} \approx 2,78 \frac{sm/sec}{v/sm}$ in nitrogen under normal conditions), the Langevin's relation being taken into account

$$b_i \sim \frac{l_i}{\bar{V}_i} \sim \sqrt{T} \qquad (13)$$

So, the values of electron concentrations n_e and positive ion mobilities b_i, determined by means of the transient electric current theory, are in good agreement with estimates obtained by other methods.

REFERENCES

1. G.G. Thomson . Conduction of Electricity through Gases. Cambridge . 1928.
2. H.A. Wilson . Rev. Mod. Phys. 3. 156. (1931).
3. А.К.Мусин. Теплофизика высоких температур (ТВТ). 2. (1964).
4. P.E. Boucher . Phys. Rev. 31. 833. (1928).
5. H.E. Banta . Phys. Rev. 33. 211. (1929).
6. S.C. Brown . Basic Data in Physics Plasmas USA. 1959.

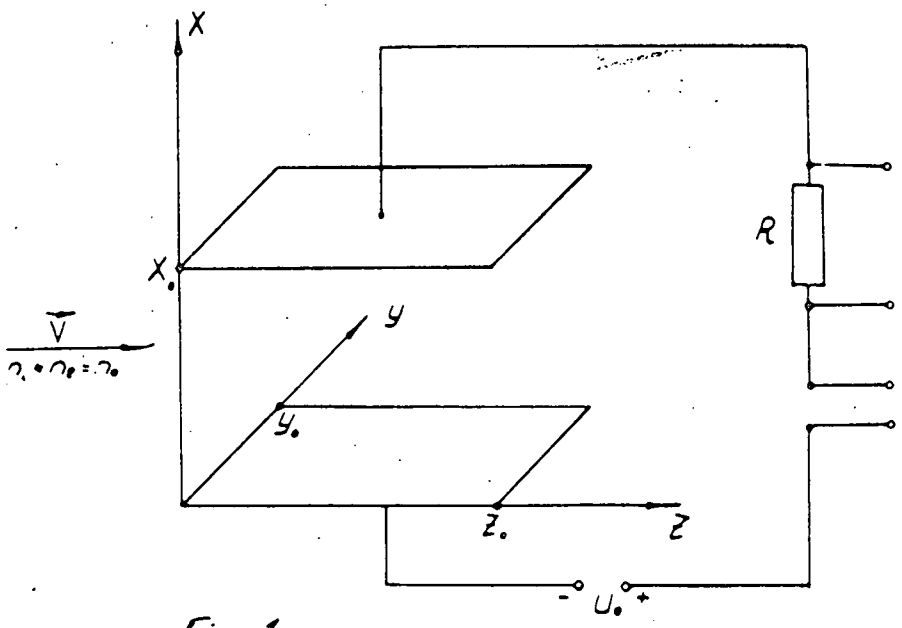

Fig:1

Fig.1. Homogeneous stream of a quasineutral plasma flows with velosity $\vec{V}$ into space between electrodes, to which a constant external voltage U_o is applied. Electrode length is - Z_o , electrode width - y_o , electrode spacing-x_o.

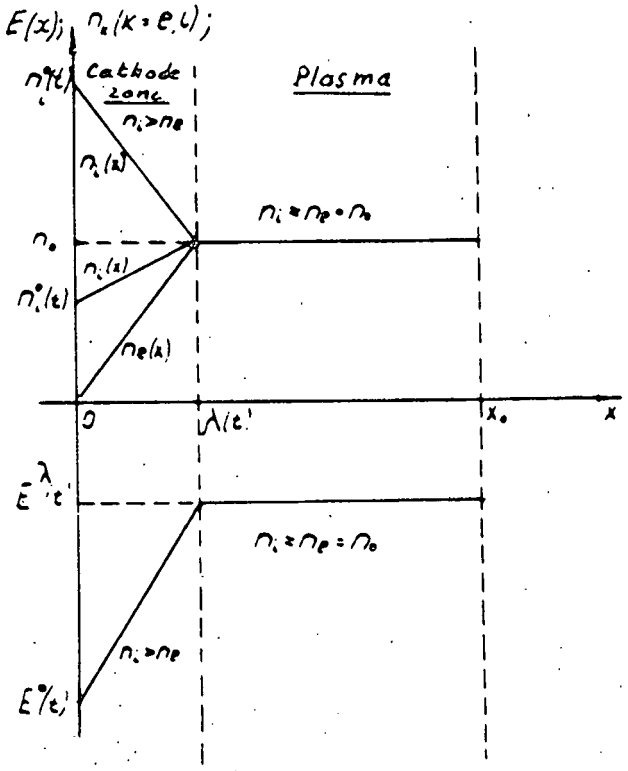

Fig: 2

Fig.2.

Functions approximating a space dependence of electron $n_e(x,t)$ and ion $n_i(x,t)$ concentrations and of electric field $E(x,t)$ in a cathode region $x \in (0,\lambda)$ and in plasma gap $x \in (\lambda, x_0)$ in a certain fixed instant $t > t_0$. Ion concentration near cathode $n_i^0(t)$ may be both greater or less than the charged particle concentration n_0 in a plasma gap.

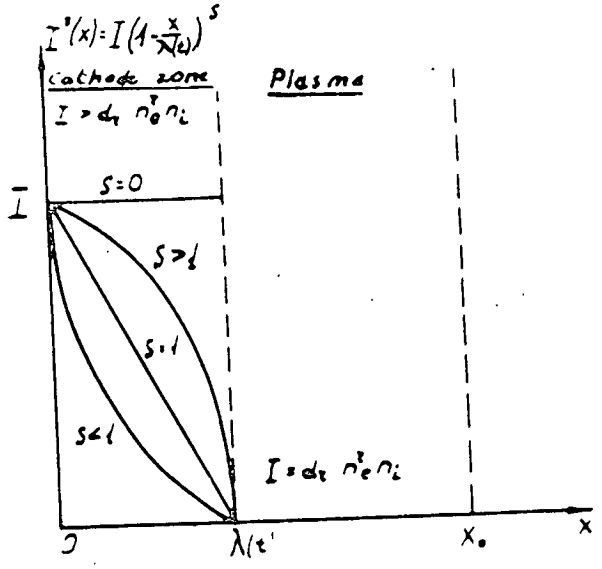

Fig:3

Fig.3.

Function approximating a space dependence of effective ionization rate $\underline{I}^{*}(x,t)=\underline{I}-\underline{\alpha}_r n_e^r n_i$ in a cathode region $x\in(0,\underline{\lambda})$ and in a plasma gap $x\in(\lambda,x_0)$ Form of the function in the cathode region is determined by value S. Due to the equality of ionization and recombination rates (ionization equilibrium) in the plasma gap the value $\underline{I}^{*}(x,t)\equiv 0$.

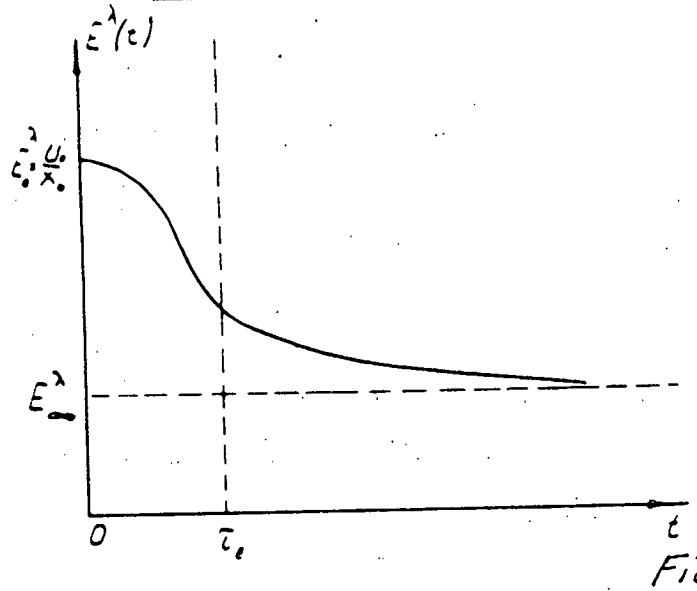

Fig:4

Fig.4.

Principal form of a function approximating a dependence of an electric field strength in a plasma gap E^{λ} upon equivalent time $t=z/v$. Relaxation time and decay factor may be found from the solution (see section 3).

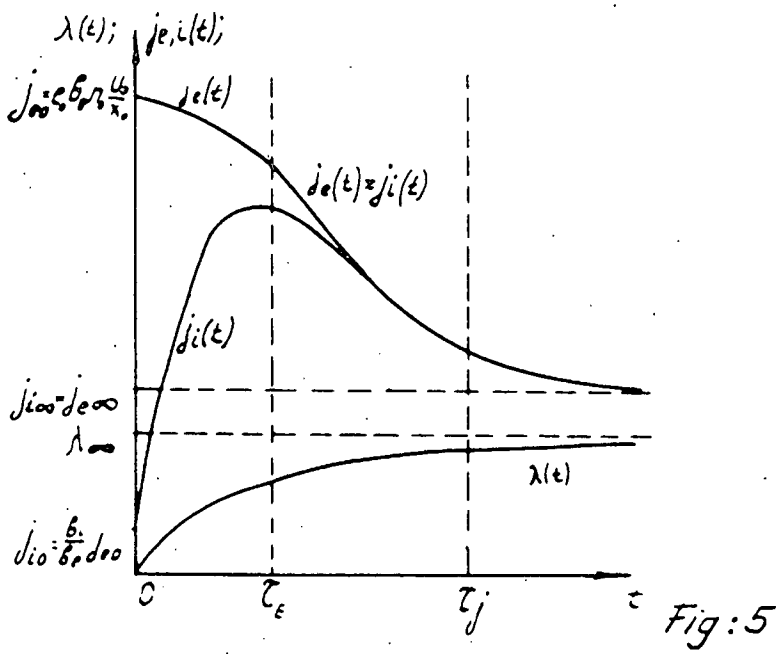

Fig:5

Fig.5.

Principal form of dependences of electronic j_e and ion j_i currents, and cathode sheath thickness λ upon equivalent time $t = z/V$. In initial setting up period $t \in (0, \tau_E)$ an electronic current j_e falls slowly and an ion current j_i rapidly increases. Ohm's law is approximately satisfied because the total current remaines approximately proportional to external voltage (see section 4.1.). In intermediate period $t \in (\tau_E, \tau_j)$ ion current passes maximum, its value approaches that of the electronic current and rapidly decreases with the latter. Ohm's law is not satisfied, ion and electronic currents depend significantly upon electron concentration in the plasma gap (see section 4.2).

When $t >> \tau_j$ (steady current period) then values j_e and j_i are equal to each other , approach their limiting value, and are determined by the ionization rate (see section 4,3).

Cathode region thickness changes monotonously, the most rapid growth occurs when $t \in (0, \tau_E)$, and asimptotically approaches its limiting value λ_∞ .

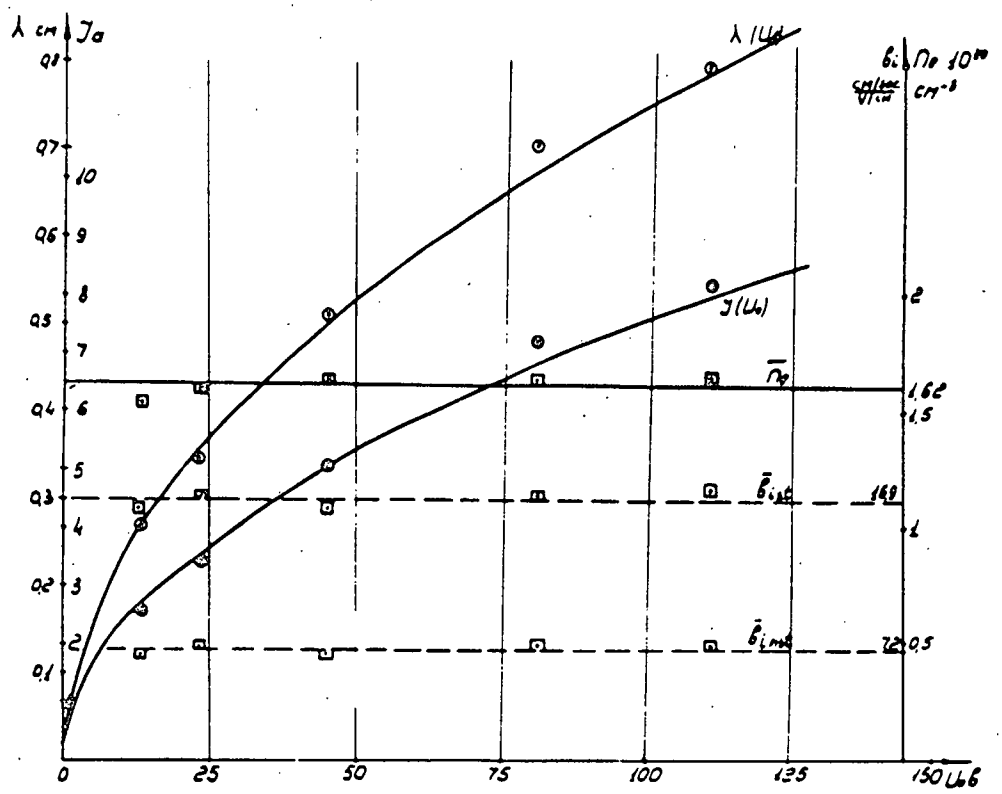

Fig: 6

Fig.6.

Results of the treatment of Boucher's [4] experiments (air flame with additive NaCl). Continuous curves (parabolas) are theoretical; they are plotted for $n_e = \overline{n}_e$ (continuous horizontal line) and $b_{i\,Na} = \overline{b}_{i\,nst}$ (lower dashed line). The upper dashed line $\overline{b}_{i\,st}$ corresponds to value $b_{i\,Na}$, obtained by the author [4] when current was assumed to be constant.

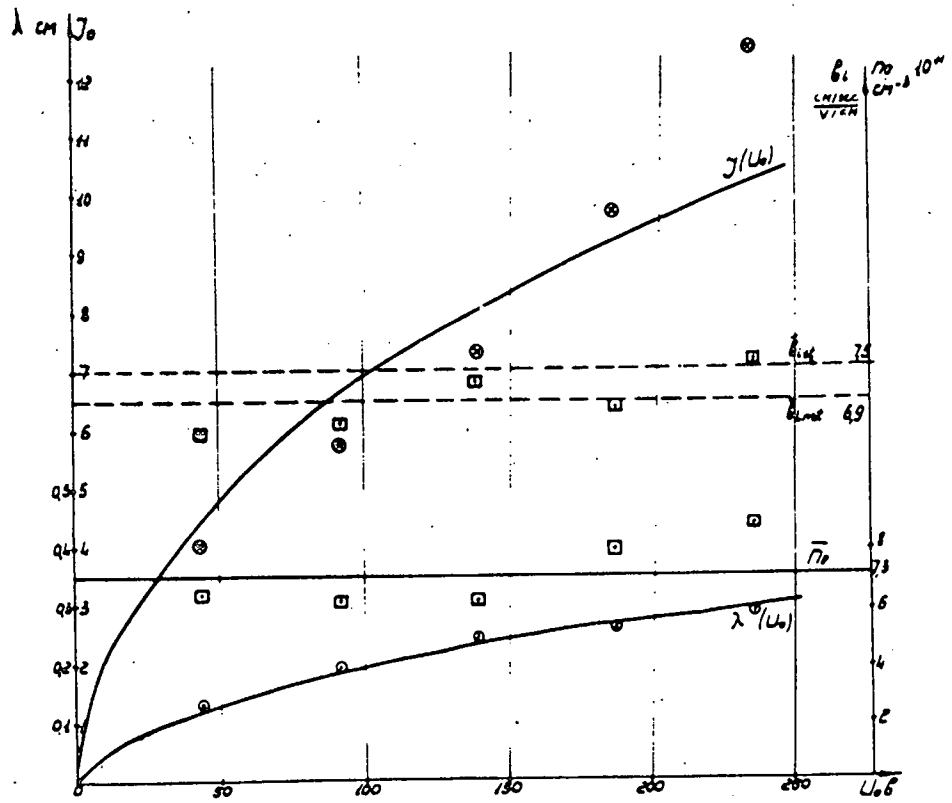

Fig: 7

Fig.7.

Results of the treatment of Banta's [5] experiments (air flame with KCl additive). Continuous curves are calculated for $n_e = \bar{n}_e$ and $b_{ik} = \bar{b}_{inst}$. A value $b_{ik} = \bar{b}_{ist}$ (the upper dashed line), obtained by the auther [5], when current was assumed to be constant, approaches value $\bar{b}_{inst}$, obtained taking account of the electric current setting up processes .

ELECTRON EMISSION IN MHD GENERATORS

D. Halász, Ch. Szendy and Ch. P. Kovács

Institute for Energy Research, Budapest, Hungary

Nomenclature

σ	gas conductivity, mhos/meter
n	number of free electrons/m^3
b_-	electron mobility, m^2 sec^{-1} $volts^{-1}$
V_j	work function, eV,
T	gas temperature, degrees Kelvin
ϱ	charge density, coulomb/m^3
r, R	radius of the sphere, m
w	velocity, meters/second
k	Boltzmann constant, $1{,}38 \times 10^{-23}$ joules/deg K
q	electronic charge, $1{,}6 \times 10^{-19}$ coulombs
E	electric field strength, volts/meter
ε_o	$\frac{1}{4\pi \cdot 9.10^9}$ $\frac{\text{coulombs}}{\text{m volt}}$
i	current density, amperes/m^2
m	electron mass, g

1. In the MHD generator the working fluid should be made to some extent /2-100 mhos/m/ conductive. As the conductivity may be expressed by

$$\sigma = n\, q\, b_- \quad \text{mhos/m} \qquad /1/$$

this can be attained if we provide for n free electrons. According to the present practice free electrons may be produced by means of thermal ionization in equilibrium. This process requires a very high temperature. The test showed, that the above conductivity values may be attained at a temperature of 2500-3100°K by seeding 1 percent of potassium to the gas.

The ionization potential of some materials:

K	4,33 V
Cs	3,90 V

The work function of these and other materials:

K	0,5 - 2,0 eV
Cs	0,7 - 1,8 eV
CsF	0,7 eV
BaO	1,0 eV

By comparing these numerical values it is obvious that the conditions of producing free electrons, as regards the required temperature, are much easier to obtain than by means of thermal ionization in the equilibrium state.

Thus, it seems worth investigating what temperature conditions occur in both cases. We assume that the selected material, with a relatively low work function /e.g. 1 eV/ and resisting to the operating temperature during a period of 1/10 to 1/100 sec, is pulverized and injected into the gas. [1]

2. Among the injected particles let us consider a sphere with a radius r_o, a work function V_j, temperature T^oK, floating in a gas. Now, let us determine how many electrons vill be emitted until the equilibrium state is attained, and in that state what will be the distribution of charges.

3. In the steady state conditon assuming only the intermolecular heat motion, the conditions for equilibrium may be determined by the following

   a/ the sum of the forces acting on an electron in any point at distance of r is equal to zero, or

   b/ the resultant of the velocities of electrons passing through the surface of a sphere of radius r /assuming spherical symmetry/ is equal to zero. It should be noted that only radial velocities are considered.

The electron acquires velocity because of two reasons:

a/ the attraction of the sphere of radius r_o becoming positive by the emission of electrons;

b/ the phenomenon of diffusion due to different charge-

Other possible effects are neglected.

Placing the origo of the coordinate-system into the centre of the sphere, the velocity caused by the electric field will be

$$w_1 = - b_- E \quad m/sec \qquad /2/$$

the velocity due of diffusion is

$$w_2 = - \frac{k\,T\,b_-}{q\,\varrho} \quad \frac{d\varrho}{dr} \quad m/sec \qquad /3/$$

In the state of equilibrium the sum of both velocities is equal to zero, that is

$$E = - \frac{k\,T}{q} \frac{1}{\varrho} \frac{d\varrho}{dr} \quad volt/m \qquad /4/$$

The system should also satisfy the Poisson's law

$$\frac{dE}{dr} + \frac{2}{r} E + \frac{\varrho}{\varepsilon_o} = 0 \qquad /5/$$

The potential of the electric field can be expressed as

$$E = - \frac{dV}{dr}$$

Therefore from /4/

$$\varrho = \varrho_o \exp \left[\frac{q\,/V_o - V/}{kT}\right]$$

where ϱ_o, V_o - are the values on the surface of radius r_o

Substituting it in the /5/, it can be written as

$$\frac{1}{r^2} \frac{d\,r^2 \frac{dV}{dr}}{dr} = - \varrho_o \exp\left[\frac{q\,/V_o - V/}{kT}\right] \qquad /6/$$

This differential equation can be solved by means of analogue computer.

4. If the temperature of the sphere of radius r_o is T^oK, the working function is V_j /volts/, than in the immediate vicinity of that sphere [2] the electron density in vacuum

$$n_o = \frac{\sqrt{2\pi\, m\, k\, T}}{\tau} \exp \left[- \frac{q\,V_j}{kT}\right] \frac{1}{\vec{}} \qquad /7/$$

$$\varrho_o = q\, n_T = \frac{i_T}{w} = \frac{i_T}{\frac{1}{2}\sqrt{\frac{2\,kT}{\pi\, m}}} \text{ - coulomb/cm}^3 \qquad /8/$$

where w is the emission velocity of electrons.

5. The investigated space is the inside of a sphere of radius R where the sum of all charges is zero. Consequently, the field strength in radius R is also zero. Thus,

$$E_R = -\left/ \frac{dV}{dr} \right/_R \equiv 0 \qquad /9/$$

This can be taken as the first initial condition of the differential equation /6/. The second condition is dealt with the charge density of electrons on the surface of radius r_o which is given by /8/.

6. In course of our investigation only one emitting spherical body /radius r_o/ has been dealt with so far, tacitly neglecting the influence between the emitting bodies being present in a great number. As we shall see in the following, with regard to the average ionization interesting us mostly in the present investigation this neglection is permissible.

Around each of the uniformly distributed spherical bodies of radius r_o, injected into the gas we imagine a concentric sphere of radius R. All these spheres fill out the whole space when arranged in the most congested manner. As is well-known, this condition is satisfied by the hexagonal arrangement when each sphere is at 12 points in contact with the surrounding spheres and the porosity, i.e. volume of space not within the spheres is 26 per cent. The phenomena are, however, definitively influenced by the events in the nearest vicinity of the solid body and the distance of both bodies from each other is generally 50 times as great as the value of r_o. On the boundary surfaces with a radius R the variables can be assumed as having identical values. Therefore we do not commit a great error if we imagine the phenomenon to proceed between the surfaces of the two concentric spheres of radius r_o and R.

7. From a high-temperature sphere of radius r_o

$$n = \int_{r_o}^{R} \frac{4 r^2 \pi \varrho \, dr}{q} \qquad /10/$$

electrons were emitted.

However, the number of molecules existing in the spherical body must be much greater than that of the emitted electrons consequently the diameter of the sphere cannot be decreased below a certain limit.

Through the emission of the electrons the sphere gets positively charged. Consequently the emitted electrons have not only to perform the work function from the molecular bond but also to overcome the potential difference between the surfaces of r_o and R .

8. As to give an idea of the quantitative conditions let us investigate the following example

$$T = 1{,}3.10^3 \ ^oK$$
$$r_o = 2{,}46.10^{-9} \ m$$
$$R = 10^{-7} \ m$$
$$V_j = 1 \ eV$$
$$\varrho_o = 4.10^5 \ coulomb/m^3$$
$$b_- = 1{,}1.10^{-1} \ m^2/volt \ sec$$

Seeded with 2 per-cent BaO.

The Eq./6/ is solved by Solatron analogue computer, so the specific charge at radius R

$$\varrho_R = 20 \ coulomb/m^3$$

The Fig shows the specific charge and the field strength in function of the radius. So it can be seen, that the required conductivity is obtained.

Even this value with certain modifications considerably

9. On the basis of the above consideration it seems possible to operate the MHD generator in a range of temperatures which the structural materials known at present can withstand.

References:

1 Mc Grath, I.A, Siddal R.G., Thring M.W.
Advances in Magnetohydrodynamics, Pergamon Press 1963. Oxford, London, New York, Paris.

2 Mc Intyre, Robert I.
Extendes Space-Charge Theory in Low-Pressure Thermoionic Converters, Journal of Applied Physics, vol. 33. No.8, Aug. 1962.

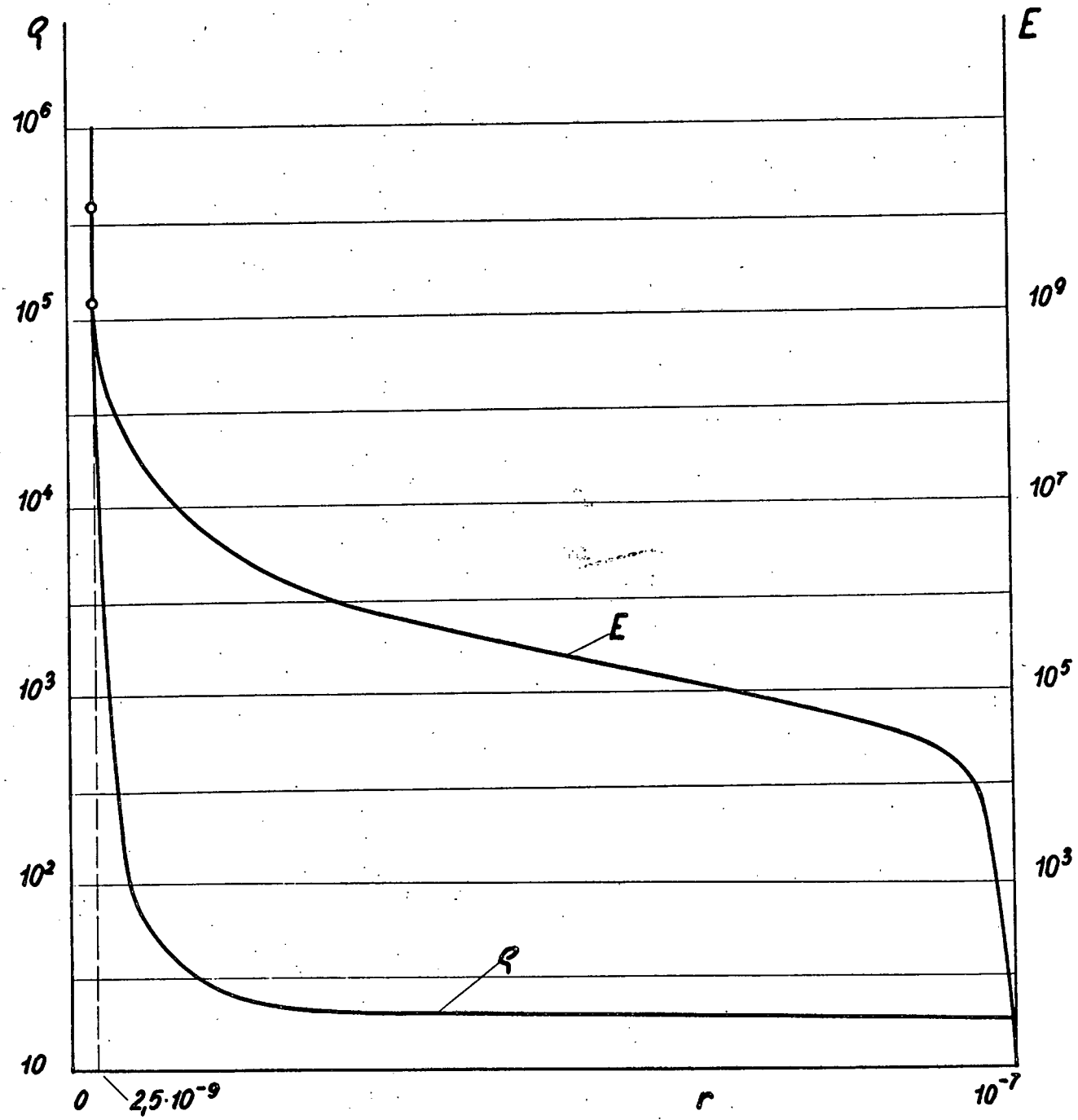

THE EXPERIMENTAL DIRECT CURRENT MHD GENERATOR OF THE OPEN CYCLE

W.S. Brzozowski, J. Dul, E. Fuksiewicz, M. Mikoś & R. Wang

Laboratory of Plasma Physics & Technology, Institut of Nuclear Research, Świerk near Warsaw, Poland

1. Introduction.

The research project on the direct conversion of thermal into electrical energy using magneto - hydrodynamic generators was first initiated in the fall of 1960 and experimental work commenced in 1961. The purpose has been to study energy conversion processes in MHD - generators and to establish their practical feasibility. After the first experiment with small power generators, performed during the 1961 and 1962 / 1,2,3 /, decision was taken to build a greater experimental unit im order to get more reliable data and to attain runs of considerable duration.

2. Open cycle direct current magnetohydrodynamic generator.

During 1963 a bigger rig was designed for thermal input power of approx. 1 MW. The general lay-out of the stand is clearly visible from the Fig.1. The facility is in the course of the final stage of assembly and it is hoped to be able, during the year to come, to evaluate some of the practical problems associated with larger scale experiments.

On completion of the programme, in 1965, it should be possible to provide a realistic assessment of the feasibility and utility of MHD electrical power generation for the future power station using oil as fuel.

In order to come as near as possible to the future practical cycle a kerosene combustion chamber was chosen charged by preheated air in a prototype heat exchanger.

During the course of erecting of the principal items of 1 MW rig / electromagnet of 20.000 Gauss, air preheater, air compressors, fuel supply installation etc./, in 1963, a programme of the preliminary investigations was carried out on smaller rigs

3. Combustion chambers.

Two combustion chambers have been built, one for 100 - 300 kW and another for 1000 kW thermal power input. Description of both designs is given in the paper, and their main features are discussed.

Small combustion chamber, 100 - 300 kW

A small rig consisting of a combustion chamber for a thermal power input of 100 kW - 300 kW, oxygen, nitrogen, air and fuel supplies was built and operated successfully during 1963. Its principal object was to study the behaviour of walls and electrodes outside the M-H-D generator itself.
This facility is shown in Fig. 2.
Kerosene was burnt in the flame of hot nitrogen and oxygen, fed separately through the plasma torch of 50 kW power. The "simulated" air has thus been preheated up to 1500°C. Additional air has also been fed by four fuel spray nozzles of air - assisted design.

Construction for high - temperature operation

The internal parts of the combustion chamber must either be capable of resisting the very high gas temperature of the combustion zone or be thoroughly cooled by air or water. We have chosen a mixed design with a ceramic flame tube made of "Refrax", with water circulating in copper tubes encircling the flame tube with an intermediate layer of "Carbofrax" cement.
The combustion chamber shown in Fig. 2 , is 154 mm long, and of 56 mm diameter.
The maximum wall temperature was kept with in a range of 1700°C.
This rather simple design proved to be very cheap in manufacturing and in maintenance, sufficiently reliable, and long - lived.
No trouble with differential thermal expansion was encountered, and no breakage observed.
The plasma torch was placed in the centre of a water - cooled copper header. Four fuel nozzles were situated circumferentially around the axis of the plasma torch outlet.
Seeding was introduced trough one nozzle as an alcohol solution of KOH. Complete stability of combustion was observed over the normal range of operating conditions, it is from 12 - 25 kg of

During the normal operation, switching off the plasma torch used to cause some instabilities, and this mode of operation had to be avoided. Special magnetic valves were embodied in the rig in order to close automatically the fuel flow to the nozzles in case of plasma torch failure.

When the seed flow was used, we experienced some trouble in that a rather great amount of slag flowed out of the outlet nozzle of the chamber.

Deposits of slag sticking to the flame tube and generator walls caused rapid corrosion of the oxide materials with subsequent spalling and cracking.

In order to get rid of that trouble, a special secondary chamber had to be designed with a slag tap in the bottom of it. The langer path of the out - going gases with several bends should guarantee that most of the slag would remain in the chamber.

Performance characteristics of small combustion chamber.

Fuel flow	12 - 25 Kg/hr
Nitrogen flow to plasma torch	10 - 12 "
Oxygen flow to plasma torch and chamber	60 - 75 "
Air to chamber and to plasma torch	35 - 50 "
Combustion intensity	0,3 - 0,5 kW/cm^3
Efficiency /including plasma torch/	0,79 - 0,88
Max.temp.of gases	2200°C - 2300°C
Max.velocity of gases	290 - 400 m/sec.
Seeding flow	5 - 20 Kg/hr / 5 percent KOH in alcohol /

Combustion chamber of 1000 kW thermal power.

The bigger combustion chamber has been designed for operation with preheated air and kerosene, No additional oxygen enrichment is to be used. Water cooling is limited only to metal parts of the header and central fuel nozzle.

A flame tube also made of "Refrax", is cooled by air. This combustion chamber has undergone preliminary investigations at another laboratory.

They included about 100 hours of operation at low power and medium temperature. At present the chamber is being prepared to run on full power for a long time. In Fig. 3 we may see the cross - section of the bigger chamber.

4. Heat exchanger.

The heat exchanger is designed for a maximum inlet gas temperature of approx. 1800°C - 2000°C; it should preheat air to 1100°C.
It is a prototype unit, and if its operation proves successful it will be further developed and multiplied.

Design conditions are as follows:

Inlet air temperature	20°C
Outlet air temperature	1000°C - 1100°C
Air flow	100 - 150 Kg/hr
Inlet air pressure	1,5 - 2,0 ata
Air pressure drop	600 mm H_2O
Inlet gas temperature	1800°C - 2000°C
Inlet gas pressure	1,05 ata
Outlet gas temperature	approx. 1600°C

Construction.

The inner tube of the heat exchanger is made of super refractory tube possessing high resistance to thermal shock, and withstanding high operating temperature as high as 1800°C.
This silicon - nitride bonded silicon carbide tube has exceptionally high thermal conductivity at high temperature / approx. 113 $\frac{\text{BTU.inch}}{\text{hr.ft}^2,^\circ\text{F}}$, or 14 $\frac{\text{Kcal}}{\text{m.hr.}^\circ\text{C}}$ at 1600°C /.

In order to increase the coefficient of heat transfer from the hot gases to the walls of the tube, special swirlers and turbulence generators have been placed in the inlet portion of the "Refrax" tube. They are made of pure stabilized zirconia bricks.
After the first experiments, special corebusters with internal air cooling will be inserted in side the tube. The cooling air will be returned to the main air flow of the recuperator.
Air enters the recuperator in the counter - flow direction, it follows a helical path formed by Nimonic L - shaped sheet tape wound around the "Refrax" tube.

One of the terminal walls of the recuperator is machined to form a flexible membrane which allows thermal movement between the tube and the outer shell; it secures, too, positive air - tight seal.

5. Electromagnet

An electromagnet for approx. 1.9 webers/m^2 has been designed and constructed.
Its main features are as follows:

pole faces	525 mm x 120 mm
maximum air gap	132 mm
power consumption	50 kW - 60 kW

The eneral view of the magnet is presented in Fig. 6
In Figs. 7 & 8 is shown the schematic diegram of powersupply and cooling system.
Fig. 9 presents magnetic induction versus current for different air gaps.

Core

A core has been fabricated from rolled sheets of approx. 1.5" ÷ 2" thickness. They have been machined and bolted together in three main parts.
The sheets are made of low carbon pure magnetic iron of the following components:

C - 0,04%; Mn - 0,014%; P - 0,015%; S - 0,023%; Cu - 0,05%; Fe - balance / "Armco E" /.
Cross - section of the magnet core is 2000 cm^2, its weight being 4200 Kg.

Coils.

The coils of the magnet have been wound from high conductivity / hollow core / copper tubes of 12 mm diameter and 4,5 mm hole diameter.
They are internally cooled by distilled water, thus providing maximum heat transfer efficiency. The coils have been insulated with glass fibre tissue of good dielectric properties and further impregnated with epoxy resin. This procedure not only adds to their electrical properties but also provides excellent

mechanical strenght.
Electrical resistance of both coils is 0,12 Ω ; weight of one coil is 420 kg.
Power is supplied by four silicon diode rectifiers of the type commonly used for welding purposes.
The maximum constant power is approx. 60 kW.
A heat exchanger included in the closed cooling loop dissipates heat to water from the mains.

Carriage.

The whole magnet is mounted on a rail carriage so that it can be rolled along the rails in the laboratory room.

6. Experiments with insulating walls.

A small rig has been constructed in order to test materials suitable for wall insulation in the conditions similar to those taking place in MHD-generators.
The facility used in our experiments is shown in Fig 10.
The hot gases pass through the test section.

In this configuration the wall temperature can easily be measured by an optical pyrometer / through holes in sidewalls /.
Some measurements have also been taken with high - temperature thermopiles.
The test section is constructed of two steel sidewalls and two ceramic / or cermetallic / elements / top and bottom /.
The steel sidewalls are water - cooled internally.
All measuring points required for heat flux calculation are provided. The above mentioned four parts are bolted together to form a rectangular housing lined with refractory slates.
Different materials were tested, as for example:

- linings moulded of SiC + 50% Al_2O_3
- bricks made of different grades of zirconia and magnesia
- bricks made of thoria
- slates made of "Refrax" and of "Refrax" coated with Al_2O_3 with plasma spray gun.

Heat flux to the walls was estimated to range from 14 W/cm^2 to 71 W/cm^2. The highest value was obtained for Refrax, the smallest for SiC + Al_2O_3 cement.

7. Electrodes

Graphite electrodes.

Experiments which were carried out at our Institute in the autumn of 1961 and during 1962 began with the use of graphite as high - temperature material for electrodes. They lasted for several minutes and enabled us to make the simple MHD - generators work and to obtain the output voltage and power as a function of the current.
In order to increase the useful life of electrodes, we used to pump methane or acetylene through pores of graphite / at a pressure of approx. 1.5 ata /.
This prodedure increased the useful life of the electrodes to 10 ÷ 15 minutes.
In some tests formation of a pyrolytic carbon layer upon the exposed surfaces of the electrodes was observed.
There was experienced some trouble caused in connection with carbon formation inside the pores of the graphite. The pores jammed, and gas flow stopped.
A new experiment using the pyrolytic graphite electrodes of considerable thickness / 5 - 10 mm / is to be carried out at a later stage.
The new electrodes are equipped with special holes for feeding methane to the exposed surfaces of the electrodes. It is hoped that this is likely to decrease the oxidation rate of the electrodes.
We have tried several other materials for the electrodes as for example:

- graphite electrodes coated pyrolytically with silicon carbide
- pure silicon carbide and silicon carbide + silicon nitride

No satisfactory solution has been found.

Zirconium oxide electrodes.

A new research programme has also been started in order to estimate the applicability of zirconium oxide for permanent electrodes.

Small specimens of 20 mm diameter and 20 mm height made of different grades of zirconia were pressed and sintered to be tested.
Platinum - rhodium wire as electrical connection has also been introduced into the sample, according to the schematic view in Fig. 11.
The specimens were tested in the air in the resistance furnace especially designed at temperatures up to 1700°C.
Some results are presented in Fig. 12.
There is some evidence, however, that zirconia may show poor resistance to the corrosive action of the potassium seeding present in the combustion gases.

Borides.

The third approach to the problem of permanent electrodes is the application of some metal borides.
Hot - pressed specimens made of titanium diboride, titanium diboride + aluminium oxide etc. have been prepared for tests. This work has just started and no results have yet been accumulated.

8. Small M-H-D generator duct.

An assembly diagram of the device is shown in Fig. 14 , and a photograph in Fig. 15.
The generator consists of three major component parts: an inlet nozzle, the M-H-D segmented electrode duct and a diffuser.
The generator itse f has a total of 8 independent transverse electrode pairs of the Faraday type.
Two electrodes of the Hall type have also been embodied in order to observe the potential difference produced at opposite ends of the duct.
The inner duct of the generator is made of thick magnesia tube Its inner diameter is approx. 1", outer diam.approx. 2".
Thermal insulation is provided by magnesia and alumina cement in subsequent layers.

The sidewalls of the housing are cooled by two water jackets situated between the magnet pole faces and the generator box. This small unit is constructed mainly for study of the performance of various types of generators / Faraday or Hall type /. Special sets of variable resistances allow fast readings to be made during operation of the unit.
The bigger unit of a rectangular cross - section is now being prepared for operation at a later stage. Its design will be based upon the results of our preliminary investigations.

References.

1. W.S.Brzozowski: "Results of the First Experiments with Small-power Magnetohydrodynamic Generators". Bulletin de L'Academie Polonaise des Sciences, Sèrie des Sciences Techniques; Vo.IX; No. 10-1961.

2. P.J.Nowacki, W.S.Brzozowski, Z.Celiński: "Experimental MHD-generator Using Combustion Gases /Gas Burner/ as Heat Source". Bulletin de L'Academie Polonaise des Sciences, Série des Sciences Techniques; Vol.X.No.5-1962

3. W.S.Brzozowski, Z.Celiński: "Plasma Generators, Plasmotrons, Arc Plasma Torches, Arc Heaters". Bulletin de L'Academie Polonaise des Sciences, Série des Sciences Techniques; Vol.X; No 5 - 1962.

4. S.Suckewer, Z.Celiński" Measurement of Plasma Velocity in the MHD Generator Duct / in Russian /. Nukleonika, 1964; Nr.IV.

Fig. 3

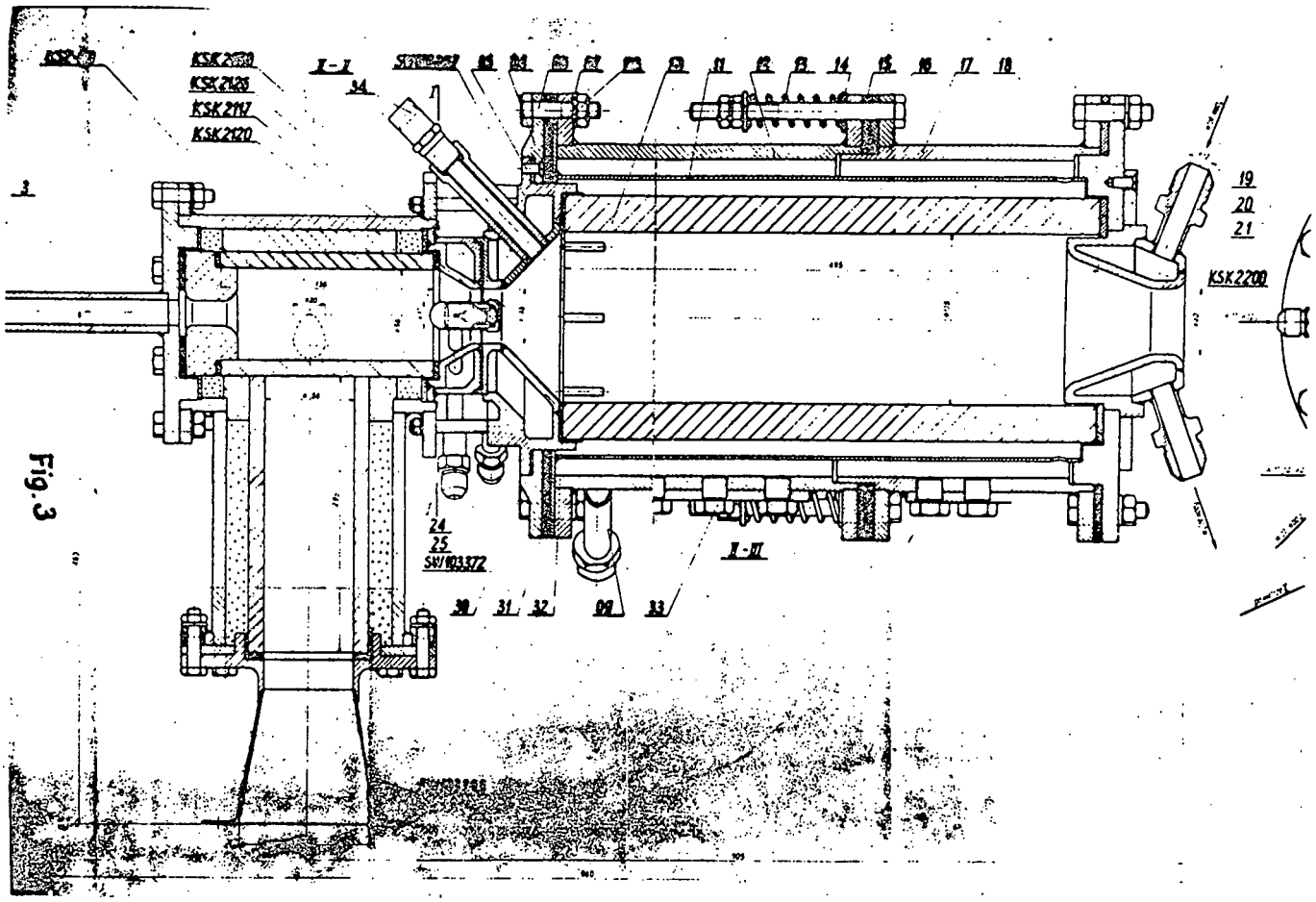

Fig. 3

Fig. 4

HEAT-EXCHANGER

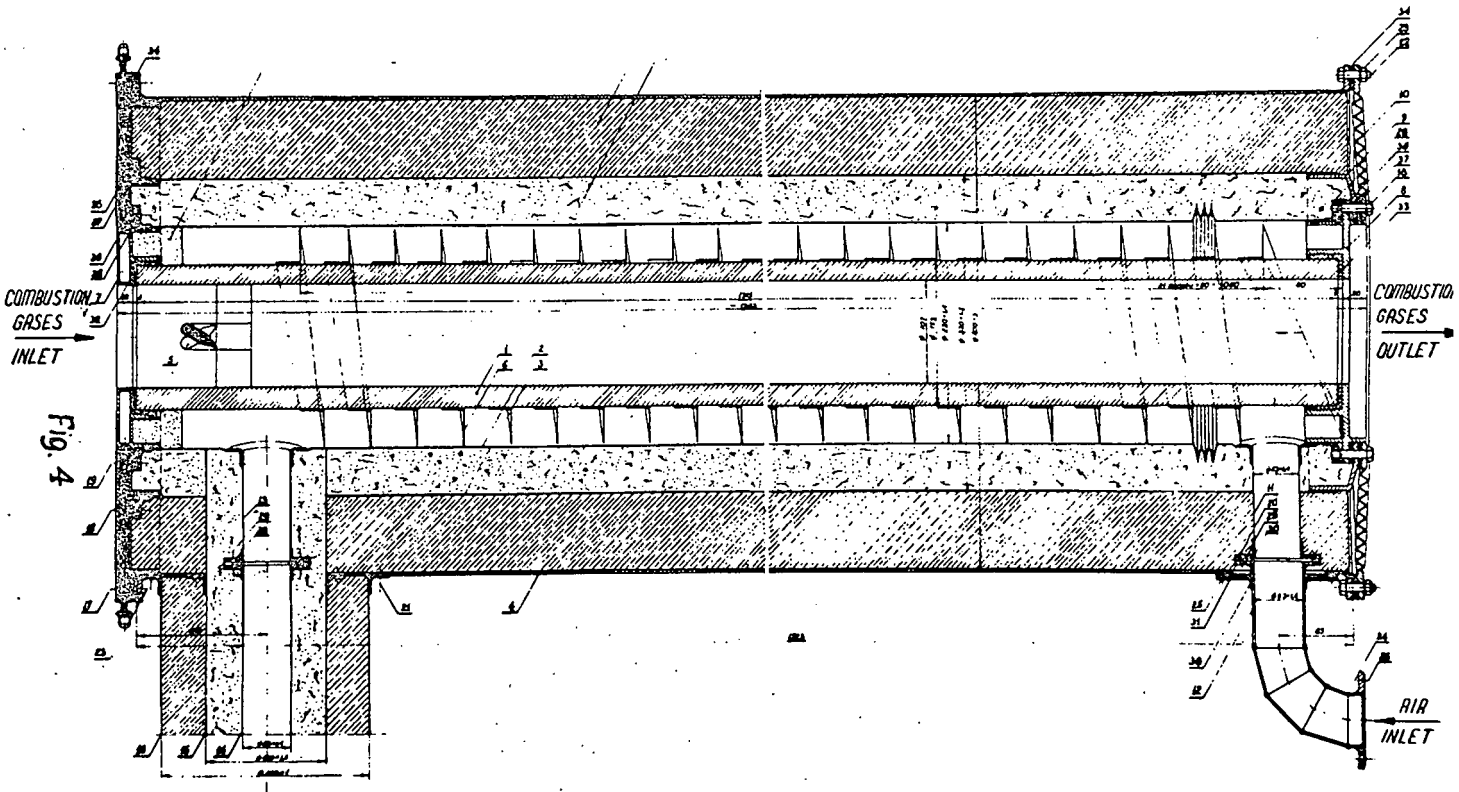

Fig. 4

GENERAL ARRANGEMENT OF M-H-D GENERATOR ASSEMBLY

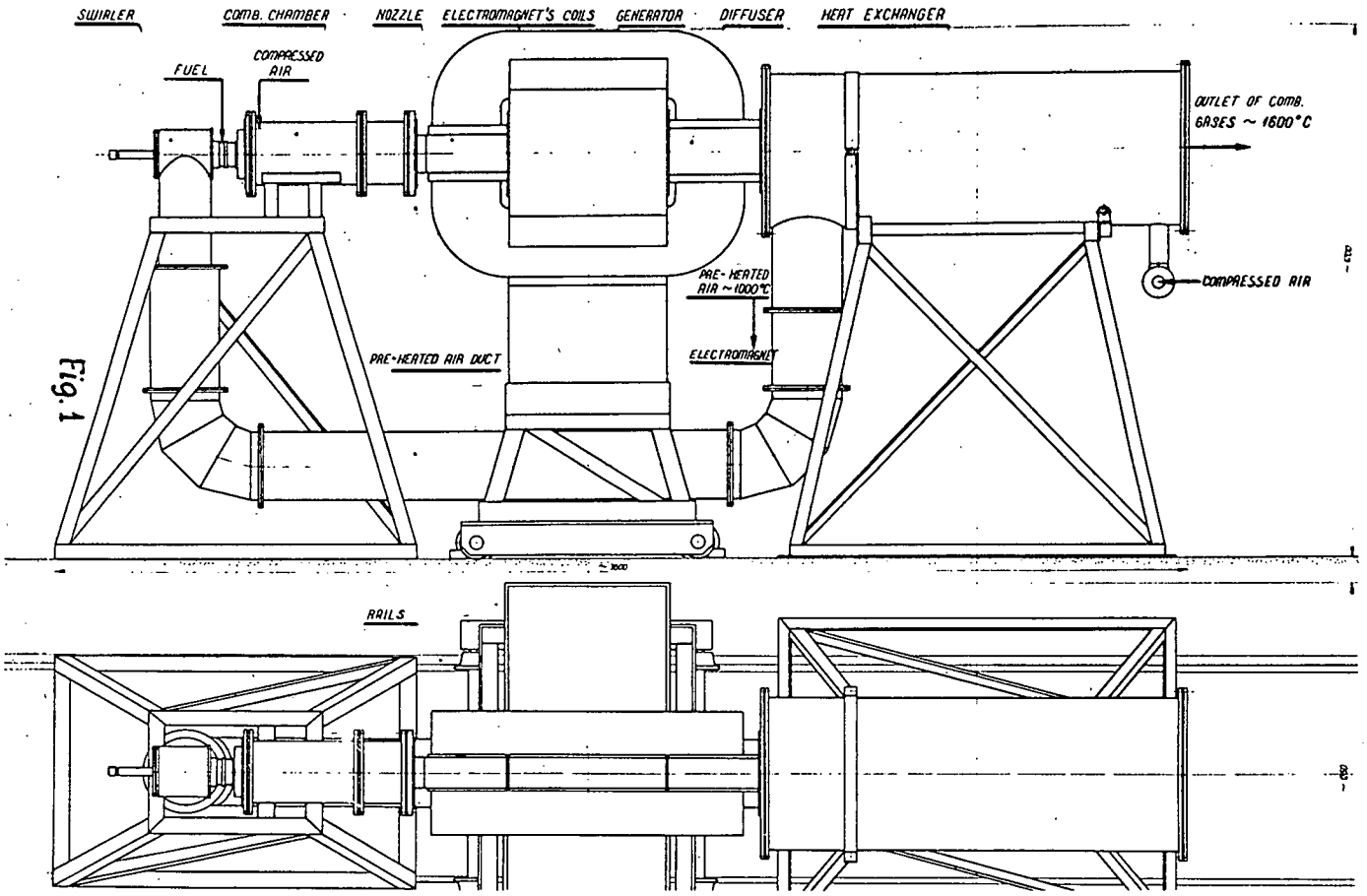

Fig. 1

Fig. 2

SMALL COMBUSTION CHAMBER (~300kW) WITH PLASMA TORCH

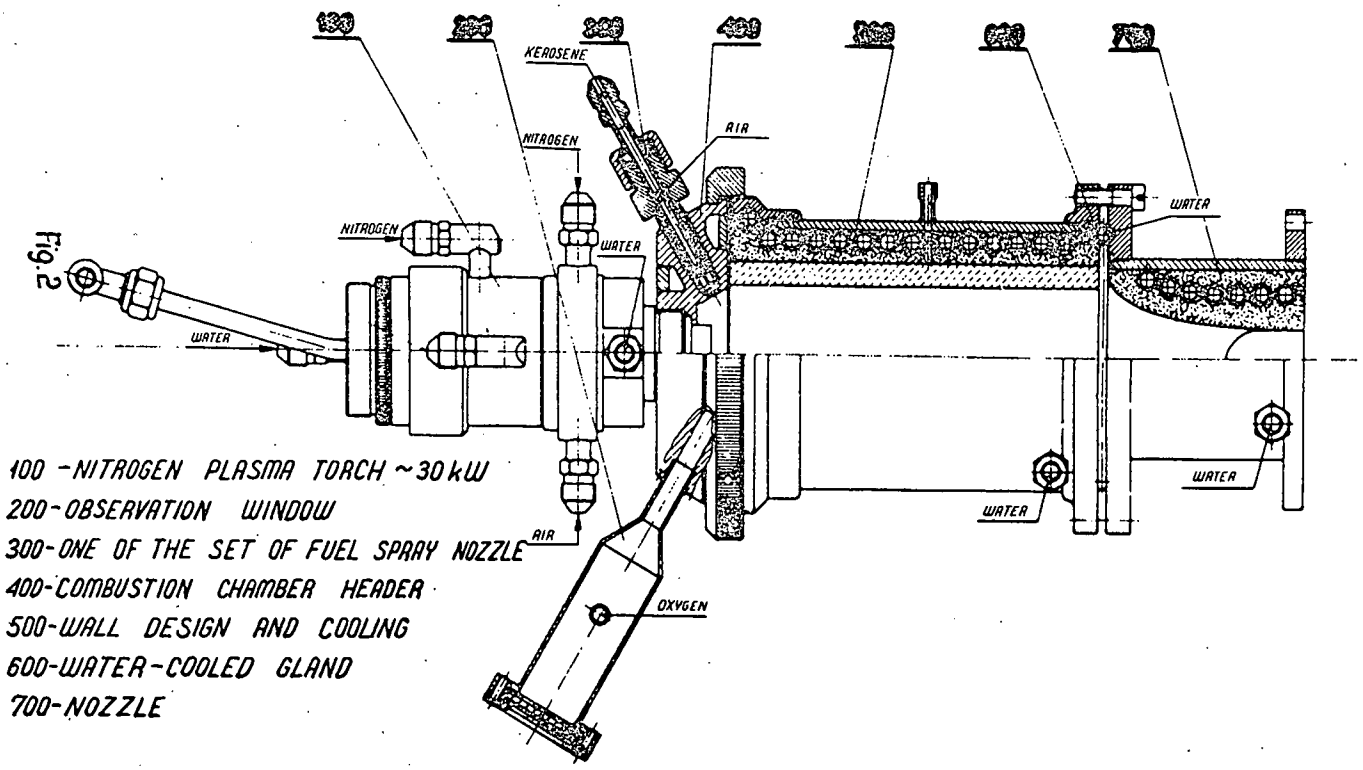

Fig. 2

100 - NITROGEN PLASMA TORCH ~30 kW
200 - OBSERVATION WINDOW
300 - ONE OF THE SET OF FUEL SPRAY NOZZLE
400 - COMBUSTION CHAMBER HEADER
500 - WALL DESIGN AND COOLING
600 - WATER-COOLED GLAND
700 - NOZZLE

Fig. 5

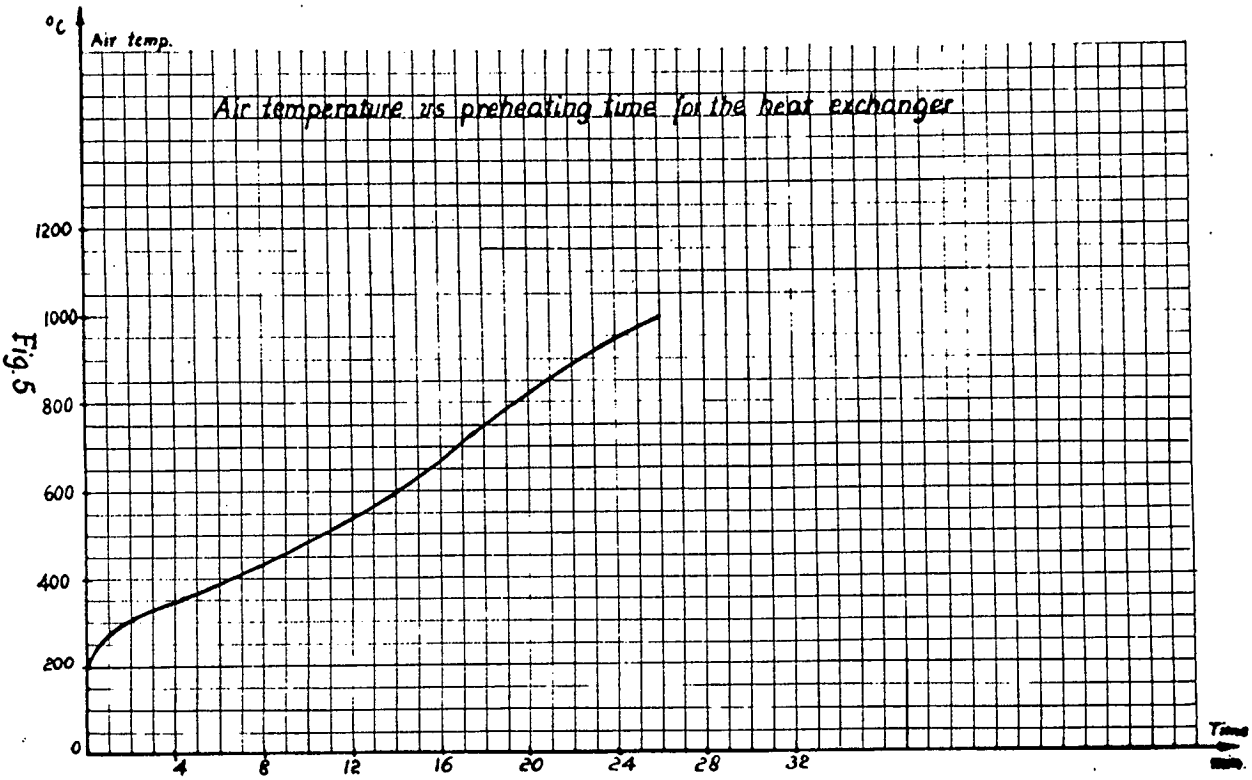

Fig. 5

Fig. 6

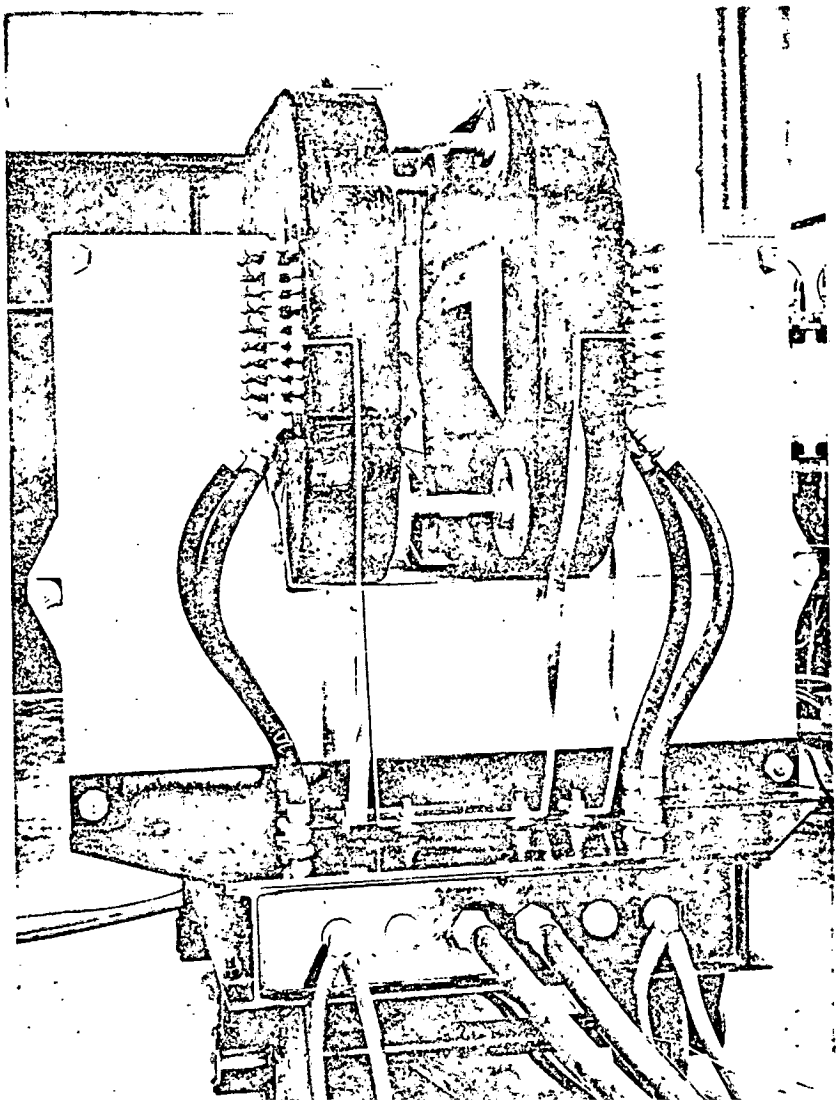

Fig. 7

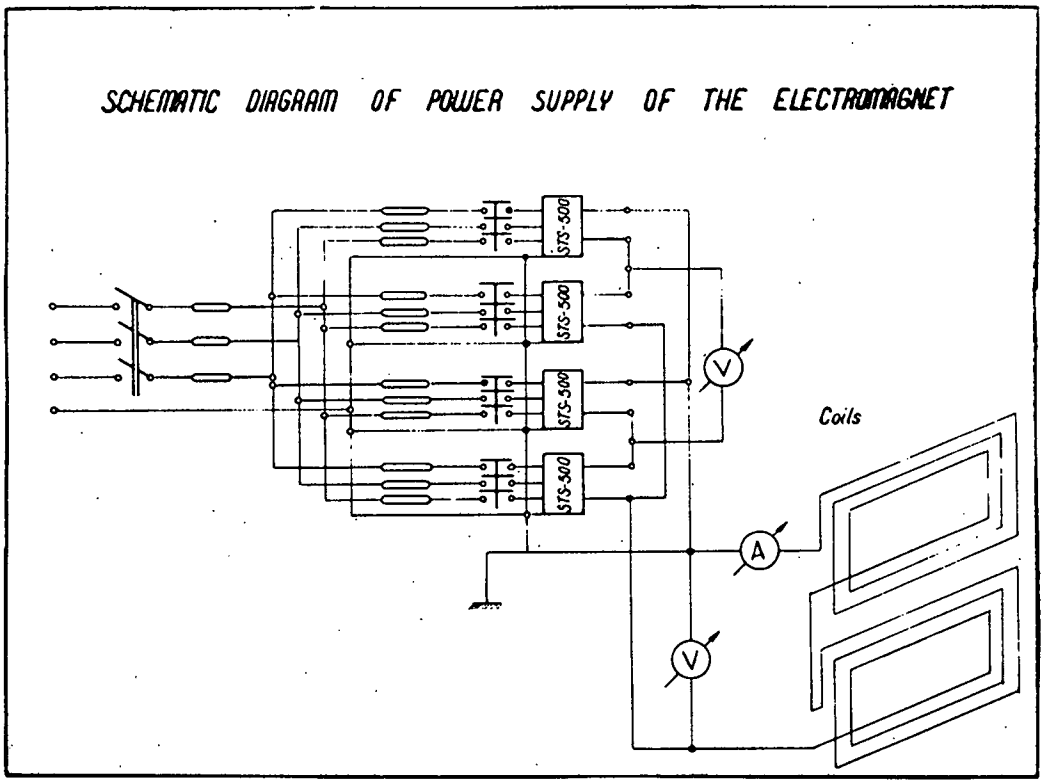

Fig. 8

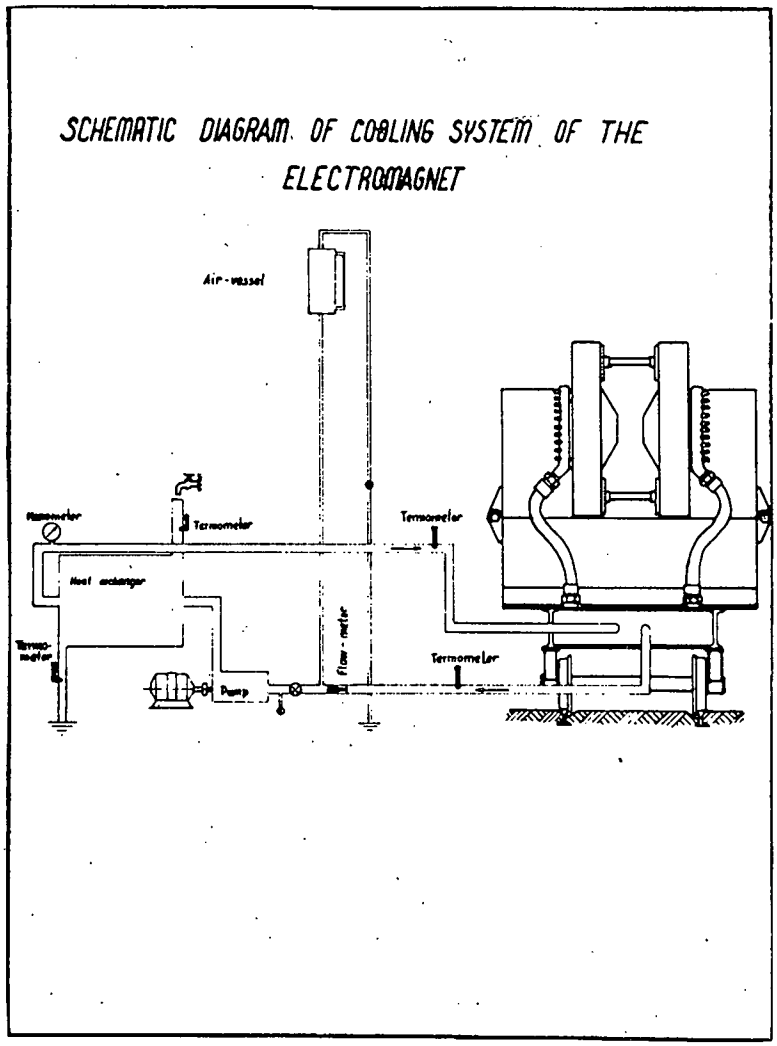

Fig. 9

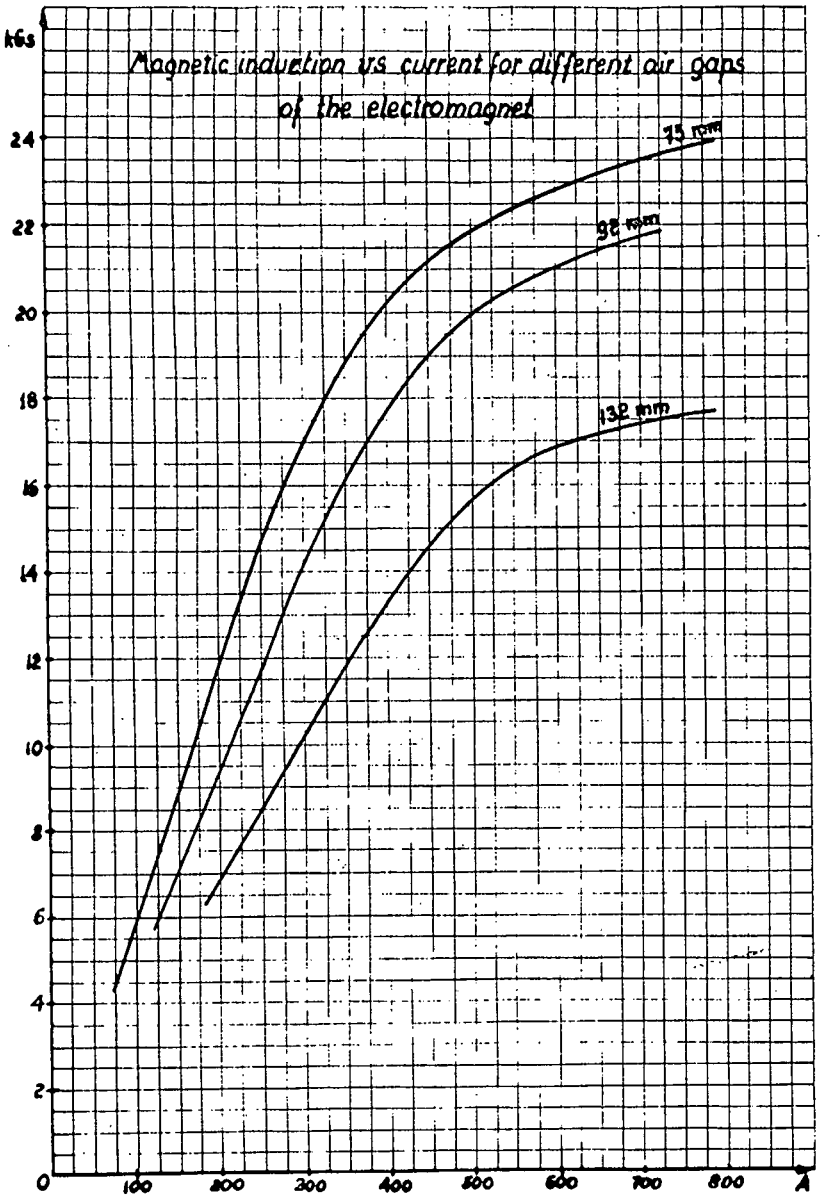

Fig. 9

Fig. 10

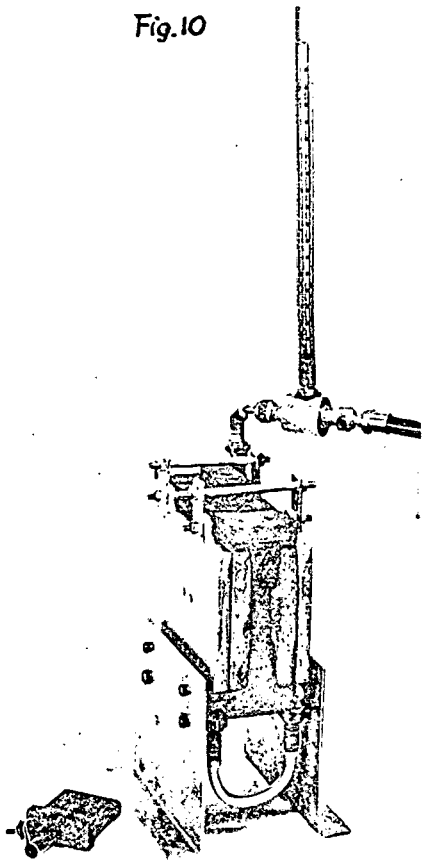

Fig. 12

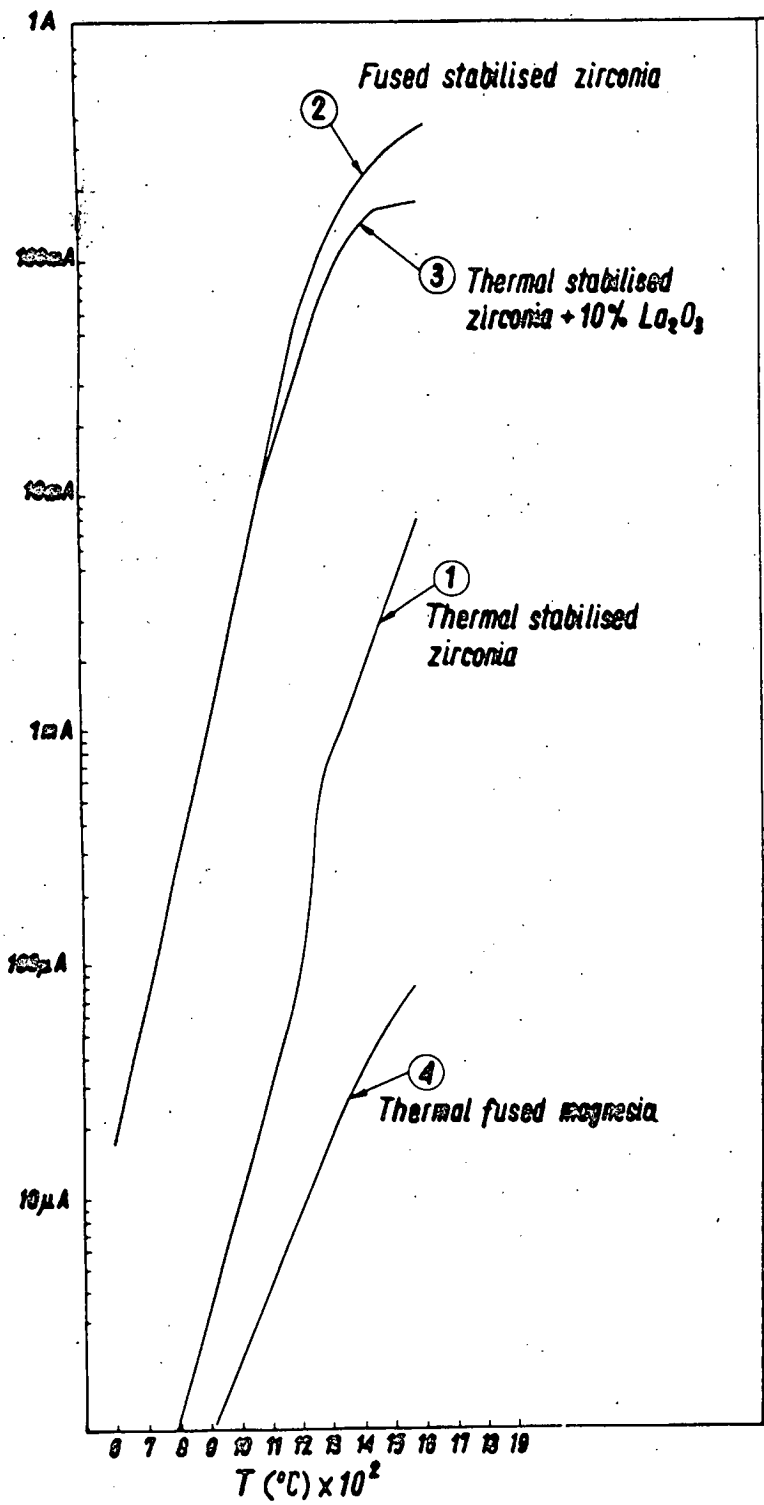

Fig. 12 Current versus temperature for different specimens (voltage kept constant 4 v)

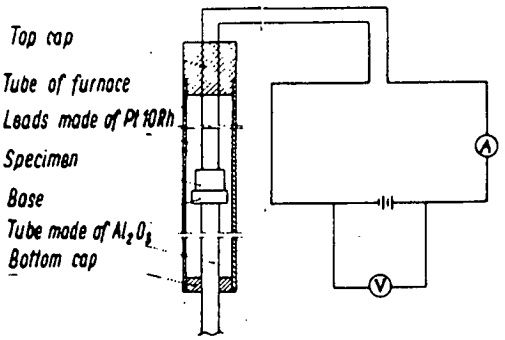

Fig. 13. Schematic view of furnace insert for electrical conductivity measurements

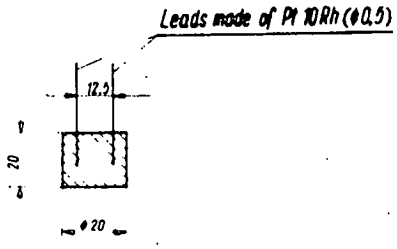

Fig. 11. Pressed and sintered specimen for electrical conductivity measurement

SMALL MHD GENERATOR DUCT

12-OBSERVATION WINDOWS
4-INLET HALL ELECTRODE
11-TRANSVERSE CURRENT ELECTRODE-
-FARADAY TYPE
4'-OUTLEL HALL ELECTRODE
1-MgO INSULATED TUBE
5-STEEL CASING
8-ALUMINIUM BOX
41-DIFFUSER CASING

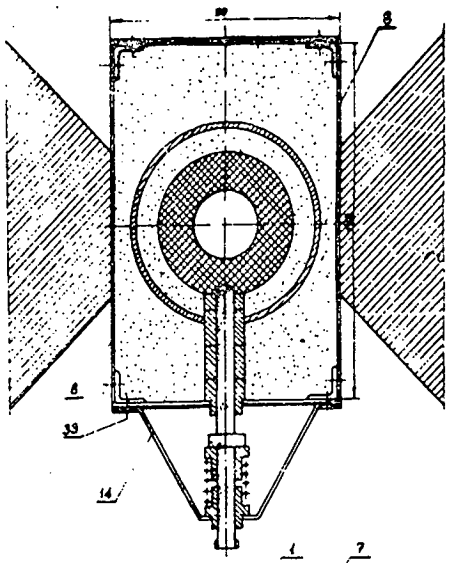

Fig. 14

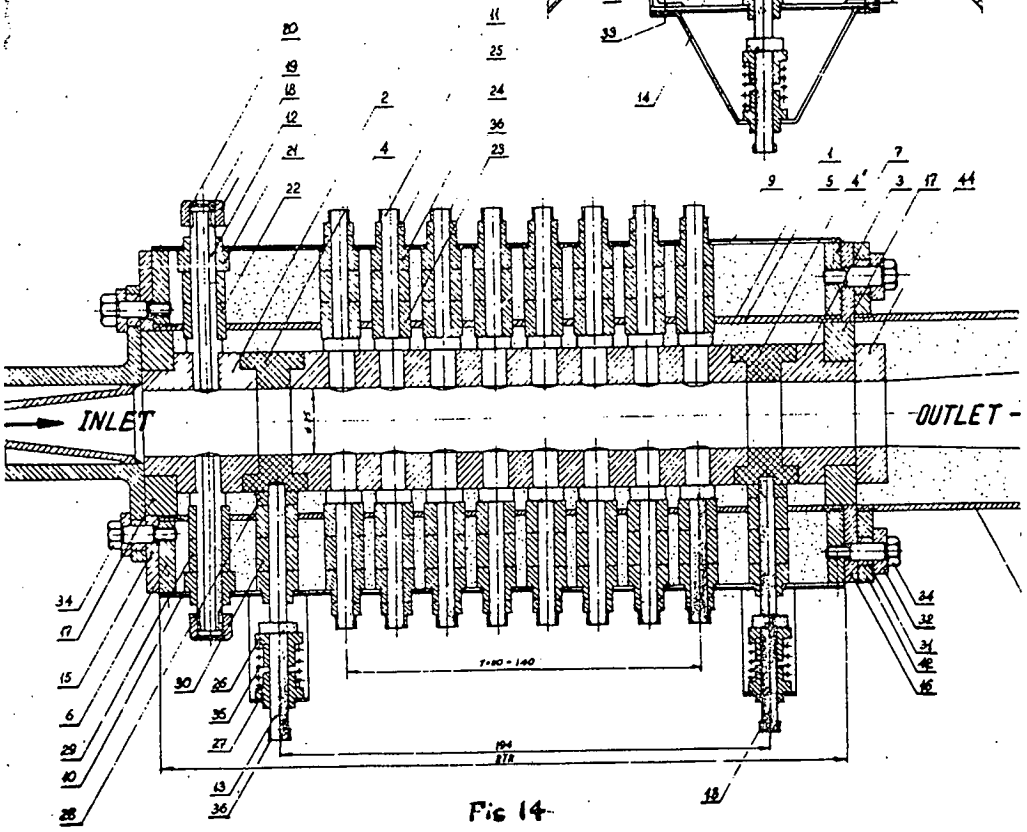

Fig 14

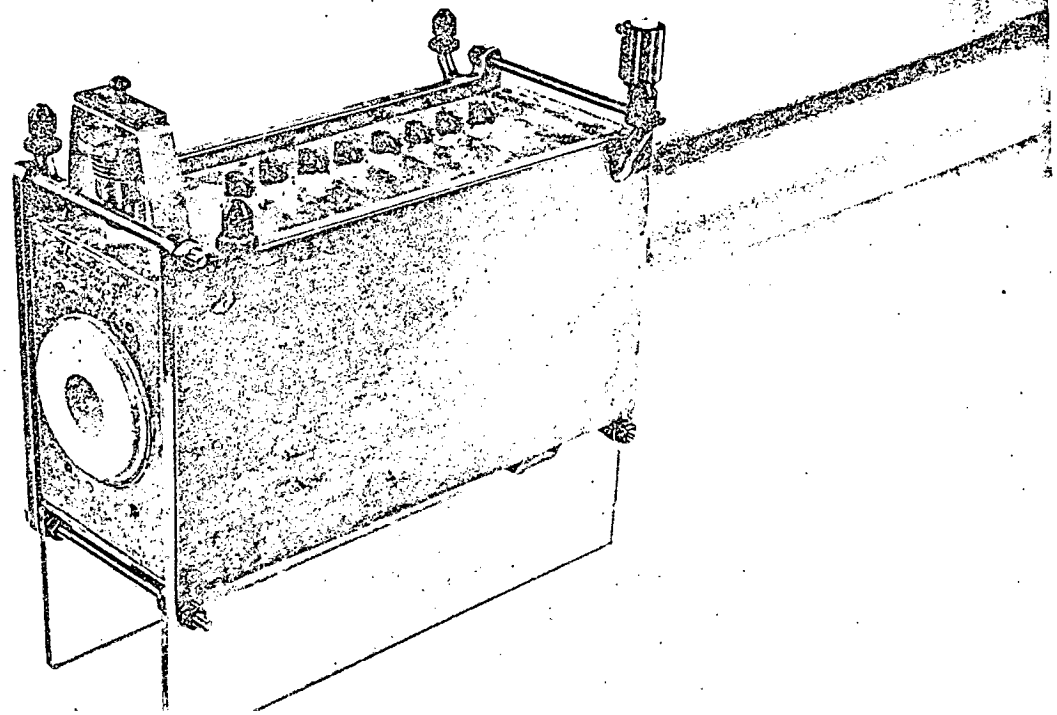

Fig. 15

ON THE PROBLEM OF OPTIMISATION OF MHD GENERATORS

A.V. Gubarev, B.Y. Shumyatsky & V.V. Brejev

Institute of High Temperatures, Moscow, USSR

The prospects for the development of any new method of energy transformation, including the magnetohydrodynamic method, are determined in the final analysis by the technical and economic indices, i.e., by the cost of one kilowatt of generated electric power. For certain specific purposes the weight and size are the most important parameters. Therefore, the study of the principal physical processes of energy transformation in M.H.D. generators and the elaboration of the principal problems of technology should be supplemented with the work to select the rational geometry of the channel, flow rates and load conditions which will ensure the optimum characteristics of the unit. The approach to the selection of the optimum parameters of a M.H.D. generator depends obviously on the purpose the unit is intended to serve and should take into account the effect produced by the generator characteristics on the parameters of the unit as a whole. On the other hand, the optimum parameters of a M.H.D. generator depend both on the principal parameters of the cycle and the choice of the thermal design of the unit. Therefore, the problem of optimisation cannot be presented today in a general form.

However, a number of important practical results can be obtained from the simplified initial premises.

The problems of optimisation of certain types of MHD generators were the subject of study in /1-6/. The optimisation was conducted with the aim of obtaining the minimum weight and size of the MHD generator and included two aspects:

1. Selection of the coefficient of electric load in a MHD generator at which the length and volume of the generator are reduced to the minimum.

2. Optimisation of the flow rates in a MHD generator channel which ensure the minimum volume and length of the generator channel at the given coefficient of electric load.

It has been shown in /6/ that with the given coefficient of electric load in the case of a variable conducti-

vity the minimum volume of the generator will be ensured if the flow rate in the channel corresponds to the maximum value of the product σu^2 (σ--gas conductivity, u--flow rate). The minimum length of the generator will be attained if the flow rate in the channel is selected from the condition of the maximum $\frac{\sigma u}{\rho}$ where ρ is the gas density. As follows from /1/ and /3/, the optimum value of electric load is not determined unambiguously. Thus, if we consider the parameters of the flow at the generator channel input as specified /1/, then the optimum value of $K_{opt} \leqslant 0.5$. Conversely, if the parameters are specified at the output of the generator channel, then $K_{opt} \geqslant 0.5$.

The common shortcoming of these investigations lies in the fact that the optimisation was performed without account being taken of the power required to drive the compressor and excite the magnetic field. Besides, the calculations disregarded the effect of the friction and heat losses on the generator characteristics. It should also be noted that the problems of optimisation of the MHD generator parameters, at which the maximum internal efficiency of the process or the maximum power of the unit are attained, have not been investigated until present time.

1.1. The useful power of the unit with a MHD generator can be determined as follows:

$$N_u = N_M + N_{s.t.u} + N_{g.t.u} - \Sigma N_c - N_{ex} - \Delta N_{pl} \qquad (1.1)$$

where N_M--power of the MHD generator;

$N_{s.t.u}$, $N_{g.t.u}$ --power of steam and gas turbine units, respectively.

ΣN_c--power required to drive the compressors in the MHD generator unit;

N_{ex}--power lost to excite the magnetic field;

ΔN_{pl}--power needed by the plant services.

For the given thermal design of the plant it can be assumed to a first approximation that the power, the weight and size factors and technical and economic indices of steam and gas turbine units are determined only from the flow of the working substance through the channel of the MHD generator and do not depend on its characteristics. The needs of the plant services are disregarded. In this case we can write

$$\Delta N_u = N_M - \Sigma N_c - N_{ex} + P \qquad (1.1a)$$

where P is the constant at the given flow of the working substance through the channel of the MHD generator (m = const) and at the specified temperature T_{02}. Consequently, with the assumptions made above, the specific output of energy $\bar{E}_{sp} = \frac{N_u}{m}$ is determined only by the cycle of the MHD generator proper (Fig. 1). It can be shown that the weight and size factors and the technical and economic indices, as well as the efficiency of the plant as a whole, will be determined in this case only by the parameters and characteristics of the MHD generator proper, i.e., the optimisation of the characteristics of the combined unit as a whole may be reduced to the optimisation of the simplest scheme of the unit with the MHD generator (Fig. 1). Then, discarding the constant P, we shall obtain:

$$N'_u = N_M - N_c - N_{ex}. \qquad (1.2)$$

1.2. The power produced in the MHD generator can be determined as follows (Fig. 1):

$$N_M = m C_{po} (T_{01} - T_{02}) - Q_w \qquad (1.3)$$

where C_{po}--average heat capacity of gas within the range of the working temperatures of the MHD generator;

$Q_w = 2\int_0^{L_g} q(\delta+h)dx$ --heat transfer to the generator walls;

$q = \alpha \Delta T_w$ --heat flux into the wall;

α --heat transfer coefficient;

$\Delta T_w = T_o - T_w$ --temperature drive;

h and δ --width and height of the channel (Fig. 2);

L_g--length of the generator channel.

The power required to drive the compressor can be found from the following relationship (Fig. 1):

$$N_c = m C_{p1} T_{1c} \frac{1}{\eta_c}\left[\left(\frac{P'_{o1}}{P'_{o2}}\right)^{\frac{\gamma-1}{\gamma}} - 1\right] \qquad (1.4)$$

where C_{p1}--average heat capacity within the range of the working temperatures of the compressor;

η_c--compressor efficiency.

The power spent to excite the magnetic field is determined from the following ratio

$$N_{ex} = \frac{j^2}{\sigma_c} \frac{G_c}{\gamma_c} \qquad (1.5)$$

where j--accepted current density in the electric magnet winding;

σ_c--conductivity of copper;

γ_c--specific weight of copper;

G_c--weight of the copper winding.

The weight of the copper winding in the simplest case of a $\square$-shaped magnetic system with steel at the constant magnetic gap is found as follows:

$$G_c = 2K\gamma_c \delta b L_g = K_1 \gamma_c L_g \frac{B\delta}{M_0 j}$$

where $b = \frac{B}{M_0 j}$ --width of the winding;

K--coefficient which accounts for the weight of the end-face sections of the winding, the number of ampereturns to overcome steel resistance, etc.

After substituting G_c in (1.5) we shall obtain

$$N_{ex} = K \frac{j}{\gamma_c} \frac{\delta B}{M_0} L_g \qquad (1.5a)$$

1.3. Utilising (1.3), (1.4) and (1.5a) we shall obtain the following expression for the useful power of the unit with a MHD generator:

$$N_u = m C_{p0} (T_{01} - T_{02}) - 2 \int_0^{L_g} \alpha \Delta T_w (\delta + h) dx - \frac{m C_{p1} T_{1c}}{\eta_c} \left[\left(\frac{P'_{01}}{P'_{02}} \right)^{\frac{\gamma-1}{\gamma}} - 1 \right] - K \frac{j}{\gamma_c} \frac{\delta B}{M_0} L_g \qquad (1.6)$$

The task of optimisation of the MHD generator parameters can be presented in the following way:

1. Let us divide termwise the right side of (1.6) by L_g, which is the length of the generator channel, and equate the derivative of the expression obtained by any of the characteristics of the parameters to zero. This will give us the optimum value of the parameter at which the specific power $\bar{N}_{uL} = \frac{N_u}{L_g}$ is at its maximum. The variational problem of optimisation may be presented in principle by a number of parameters.

2. Let us divide termwise the right side of (1.6) by the useful volume of the generator channel

$$V_g = \int_0^{L_1} \delta h dx \qquad (1.7)$$

and, equating the respective derivatives to zero, find the optimum values of the sought-for parameters at which $N_{uv} = \frac{N_u}{N_g}$ is at its maximum.

3. Let us divide termwise the right side of (1.6) by the mass flow rate of gas in the generator channel and, equating the derivatives to zero, determine the optimum value of any of the parameters which corresponds to the maximum value of the useful energy obtained from one kg of the mass.

$$\overline{E}_{sp} = \frac{N_u}{m} \qquad (1.8)$$

The first two presentations of the optimisation problem are related to the weight and size factors of the unit with a MHD generator.[x] It should be noted that the optimisation both by the length and the volume of the generator does not determine the optimum value by the weight and size factors of the unit with sufficient accuracy. However, it is extremely difficult to indicate a more accurate method of optimisation of the weight and size factors, which would permit an elementary analysis.

The optimisation of the parameters of the MHD generator in the third presentation of the problem in the case of the specified value of $\Delta T_M = T_{o1} - T_{o2}$ corresponds to the optimum value of the unit efficiency. If the power

---

[x] This assertion is true if the weight of the MHD generator with a magnetic system considerably exceeds the weight of the other elements of the unit or when the variations of any of the parameters do not affect their weight and size factors.

spent to create a magnetic field and the heat transfer to the generator walls are negligibly small, such optimisation can be reduced to finding the maximum of the internal efficiency of the energy transformation process in the generator.

It should be stressed that in the case of more complete presentation of the problem of determining the maximum of the unit efficiency we shall require variation of the parameters at the output of the MHD generator channel and, in a general case, the value P in (1.1a) cannot be assumed constant. The solution of such a problem, and of the problem of determining the optimum value by the technical and economic indices of the electric power plant as a whole, is rather difficult in the form accessible for analysis and requires a large number of variational calculations.

The general approach to the problem of optimisation of the parameters of the MHD generator was discussed above. To solve this problem we must establish the relationships between the parameters of the flow in the MHD generator channel, its load characteristics and geometrical dimensions. The main difficulties of optimisation accrue from the complex and multi-valued nature of these relationships. Therefore, the variational problem must in a general case be presented with many degrees of freedom. In our further exposition we shall confine ourselves to establishing these relationships on the basis of the quasi-one-dimensional theory and, making certain assumptions, shall reveal the qualitative aspect of the problem of optimisation of the principal operating characteristics of MHD generators. In conclusion we shall give some results of the calculations performed on a type M-20 computer.

2.1. Accepting certain assumptions, the flow of gas in the MHD generator channel can be described by the following system of equations:

1. Continuity equation

$$\rho u \delta_h = m = \text{const.} \tag{2.1}$$

2. Momentum equation

$$\rho u du + dp = -\left[(1-\kappa)\sigma u B^2 + \xi \frac{\rho u^2}{2 D_{eq}}\right] dx \tag{2.2}$$

3. Energy equation

$$m C_p dT + m u du = -\left[\kappa(1-\kappa)\sigma u^2 B^2 \delta_h + 2\alpha(\delta + h)\Delta T_w\right] dx \tag{2.3}$$

4. Equation of state

$$P = \rho R T \tag{2.4}$$

The following notation is used here:

ξ--coefficient of friction;

$D_{eq} = \frac{2\delta h}{\delta + h}$ --equivalent diameter of the channel;

R--gas constant;

$\kappa = \frac{E}{uB}$ --coefficient of electric load;

E--electric field intensity;

$T_0 = T + \frac{u^2}{2c_p}$ --total temperature of gas flow.

The change in the conductivity of gas σ depending on the thermodynamic parameters of the flow can be represented to a first approximation as follows

$$\sigma = C_1 e^{\alpha_1 T} p^{\beta} \tag{2.5}$$

or

$$\sigma = C_2 T^{\alpha_2} p^{\beta} \tag{2.5a}$$

The heat transfer coefficient α will be determined from the known formulas

$$Nu_f = 0.023 \, Re_f^{0.8} \, Pr_f^{0.4} \tag{2.6}$$

where the criteria

$$Nu_f = \frac{\alpha D_{eq}}{\lambda_f} \quad \text{and} \quad Re_f = \frac{\rho u D_{eq}}{\mu_f}$$

are determined by the usual methods.

The system of equations (2.1) (2.6) is not complete and to solve our problem we must establish additional relationships for certain parameters which enter into the system. In our further exposition the following parameters will be assumed constant along the channel length for the sake of simplicity:

$$n,\ B,\ k,\quad \Delta T_w = T_0 - T_w,\quad \varkappa = \delta/h = 0.5$$

Then, we have

$$\rho u \delta^2 = \frac{m}{2} = \text{const} \tag{2.7a}$$

$$dp = -\left[(1-\kappa)\sigma u B^2 + \xi \frac{3}{4}\sqrt{\frac{2\rho u}{m}}\,\rho u^2\right] dx \tag{2.7b}$$

$$m C_p dT = m C_p dT_0 = -\left[\kappa(1-\kappa)\frac{\sigma u B^2}{\rho} m + 6\alpha\sqrt{\frac{m}{2\rho u}}\,\Delta T_w\right] dx \tag{2.7c}$$

2.2. Let us consider the limiting cycle of the unit with a MHD generator when the temperature drop used in the generator $\Delta T_0 \to 0$. Then the power of the MHD generator will be

$$\Delta N_M = \kappa(1-\kappa)\frac{\sigma u B^2}{\rho} m \Delta x = m C_p \Delta T_0 - 6\alpha\sqrt{\frac{m}{2\rho u}}\,\Delta T_w \Delta x \tag{2.8}$$

The pressure drop over the length of the generator

$$\Delta x = \frac{m C_p \Delta T_0}{\kappa(1-\kappa)\frac{\sigma u B^2}{\rho} m + 6\alpha\sqrt{\frac{m}{2\rho u}}\,\Delta T_w} \tag{2.9}$$

is determined as follows

$$\Delta P = P_1 - P_2 = \left[(1-\kappa)\sigma u B^2 + \frac{3}{4}\xi \rho u^2\right]\sqrt{\frac{2\rho u}{m}}\,\Delta x \tag{2.10}$$

and after appropriate transformations, assuming that the pressure loss between the channel and the compressor is equal to zero, we shall obtain the following expression

for the compressor power:

$$\Delta N_c = \frac{m C_p T_{1c}}{\eta_c}\left[\left(1+\frac{\left(1+\frac{\gamma-1}{2}M_1^2\right)^{\frac{\gamma}{\gamma-1}}}{P_0}\left((1-\kappa)\sigma u B^2+\frac{3}{4}\xi\rho u^2\sqrt{\frac{2\rho u}{m}}\right)\Delta x\right)^{\frac{\gamma-1}{\gamma}}-1\right] \qquad (2.11)$$

Thus, after substituting (2.8) and (2.11) in (1.2) we shall obtain

$$\Delta N_u = \kappa(1-\kappa)\frac{\sigma u B^2}{\rho} m\Delta x - \frac{m C_p T_{1c}}{\eta_c}\left[\left(1+\frac{\Delta P_0}{P_0}\right)^{\frac{\gamma-1}{\gamma}}-1\right] - K_1\frac{j}{\sigma_c}\frac{B}{M_0}\sqrt{\frac{m}{2\rho u}}\Delta x \qquad (2.12)$$

where

$$\Delta P_0 = \left(1+\frac{\gamma-1}{2}M^2\right)^{\frac{\gamma}{\gamma-1}}\left[(1-\kappa)\sigma u B^2+\frac{3}{4}\xi\rho u^2\sqrt{\frac{2\rho u}{m}}\right]\Delta x$$

2.3. It follows from (2.12) that with the given parameters of the flow at the input of the MHD generator channel, with the length Δx, the useful power of the unit depends on the rate of flow u, the coefficient of electric load and also on the characteristics of the magnetic system field induction B, copper conductivity σ_c and the current density in the winding. The optimum characteristics of the MHD generator can be obtained by equating the respective derivatives to zero:

$$\frac{d}{d\kappa}(\Delta N_u)=0,\ \frac{d}{du}(\Delta N_u)=0 \qquad (2.13)$$

Let us consider some particular cases.

1. Let $\Delta N_M \gg \Delta N_c$ which holds at $\frac{T_{01}}{T_{1c}} \gg 1$. Then $K_{opt} = 0.5$. Equating $\Delta N_u = 0$, we shall find the value of the induction B at which the MHD generator ensures the power spent on excitation:

$$B \geq K_1\frac{j}{\mu_0\sigma_c}\frac{1}{\sigma u^2\kappa(1-\kappa)}\sqrt{\frac{\rho u}{2m}} \qquad (2.14)$$

2. Let $\Delta N_M \gg \Delta N_c$ and, besides, $\Delta N_M \gg \Delta N_{ex}$. Then the optimum value of the flow rate can be found from

$$\frac{d}{du}\left(\frac{\sigma u}{\rho}\right)=0 \qquad (2.15)$$

Assuming the power dependence of the conductivity on the flow parameters (2.5a) and remembering that the velocity of sound $a = \gamma \frac{p}{\rho}$ we reduce (2.15) to the form

$$\frac{d}{dM}\left[M\left(1+\frac{\gamma-1}{2}M^2\right)^{\frac{2-\alpha-\gamma(1+\beta)}{\gamma-1}}\right]=0$$

Hence, the optimum value of Mach number

$$M_{opt}=\sqrt{\frac{2}{\gamma-1}\,\frac{1}{2\left(\alpha+(1+\beta)\frac{\gamma}{\gamma-1}-2\frac{1}{\gamma-1}\right)-1}} \qquad (2.16)$$

Consequently, we can assume in a sufficiently narrow temperature range that the optimum value of the flow rate in the generator channel is constant /6/ and does not depend on its load characteristics.

If the power spent on excitation cannot be neglected the optimum Mach number will be

$$M'_{opt} > M_{opt} \quad \text{at} \quad M_{opt} < 1$$

$$M'_{opt} < M_{opt} \quad \text{at} \quad M_{opt} > 1 \qquad (2.17)$$

3. If none of the terms in (2.12) may be neglected optimisation in an analytical form becomes difficult. However, a number of qualitative conclusions can be made from (2.12). As was shown above, the maximum value of $\Delta N_M - \Delta N_{ex}$ is attained at K = 0.5. The power required to drive the compressor decreases monotonously when K increases from 0 to 1. Therefore, the useful power of the unit with a MHD generator reaches its maximum when K > 0.5. Fig. 3 illustrates the effect of K on the useful power of the unit.

2.4. Let us dwell briefly on the choice of the operating conditions of the generator which will ensure the maximum take-off of power from the unit of the channel volume

$$\Delta V_g = \frac{m}{\rho u}\Delta x \qquad (2.18)$$

Then, the specific power of the unit will be

$$N_{uv} = \frac{\Delta N_u}{\Delta V_g} = K(1-K)\sigma u^2 B^2 - \frac{\rho u}{\Delta x}\frac{C_p T_{1c}}{\eta_c}\left[\left(1+\frac{\Delta P_0}{P_0}\right)^{\frac{\gamma-1}{\gamma}}-1\right] - K_1 \frac{\dot{\sigma}}{\sigma_c}\frac{B}{\mu_0}\sqrt{\frac{\rho u}{2m}} \qquad (2.19)$$

When $\Delta N_c \ll \Delta N_M$, optimisation by the coefficient of electric load gives the same result K = 0.5. If, besides, $\Delta N_{ex} \ll \Delta N_M$ the optimum value of the flow rate can be determined from

$$\frac{d}{du}(\rho u^2) = 0$$

Hence, with the power dependence of σ (2.5a) we obtain

$$M_{opt} = \sqrt{\frac{2}{\gamma-1}\frac{1}{\alpha+(2+\beta)\frac{\gamma}{\gamma-1}-\frac{\gamma+1}{\gamma-1}}} \qquad (2.20)$$

Accounting for the power spent on excitation the result will be reversed (2.17). Indeed, it follows from (2.19) that

$$M'_{opt} < M_{opt} \quad \text{at} \quad M_{opt} < 1$$
$$M'_{opt} > M_{opt} \quad \text{at} \quad M_{opt} > 1 \qquad (2.21)$$

2.5. Above we considered the problems of selecting the operating conditions for MHD generator which ensured the minimum weight and size of the unit. For stationary electric power installations the weight and size factors determine the capital outlay and their efficiency becomes the principal factor.

Let us consider the problem of selecting the operating conditions for MHD generator which ensure the maximum efficiency of the unit. For this purpose, we shall reduce (2.12), with account taken of (2.9), to the following form

$$\Delta N_u = m C_p \Delta T_0 \left[\frac{\kappa(1-\kappa)\frac{\sigma_u B^2}{\rho} m - K \frac{j}{b_c} \frac{B}{M_0} \sqrt{\frac{m}{2\rho u}}}{\kappa(1-\kappa)\frac{\sigma_u B^2}{\rho} m + 6\alpha \sqrt{\frac{m}{2\rho u}} \Delta T_w} \right] - \frac{m C_p T_{1c}}{\eta_c} \left[\left(1 + \frac{\Delta p_0}{p_0}\right)^{\frac{\gamma-1}{\gamma}} - 1 \right] \quad (2.22)$$

where

$$\Delta p_0 = m C_p \Delta T_0 \left(1 + \frac{\gamma-1}{2} M^2\right)^{\frac{\gamma}{\gamma-1}} \frac{(1-\kappa)\sigma_u B^2 + \frac{3}{4} f \rho u^2 \sqrt{\frac{2\rho u}{m}}}{\kappa(1-\kappa)\frac{\sigma_u B^2}{\rho} m + 6\alpha \sqrt{\frac{m}{2\rho u}} \Delta T_w}$$

A detailed analysis of (2.22) is extremely complicated. Therefore, let us first consider a case in which the effect of friction, heat transfer to the wall and the power spent on exciting the magnetic field are disregarded. Then

$$\Delta \bar{E}_{sp} = \frac{\Delta N_u}{m} = C_p \Delta T_0 - \frac{C_p T_{1c}}{\eta_c} \left\{ \left[1 + \frac{\gamma}{\kappa(\gamma-1)} \left(1 + \frac{\gamma-1}{2} M^2\right) \frac{\Delta T_0}{T_0} \right]^{\frac{\gamma-1}{\gamma}} - 1 \right\} \quad (2.23)$$

Hence, it follows that with the given parameters of the cycle the efficiency of the unit will be determined only by the coefficient of electric load K. Equating the derivative from (2.23) by K to zero we shall obtain:

$$\frac{1}{\kappa^2 + \kappa \frac{\gamma}{\gamma-1}\left(1 + \frac{\gamma-1}{2} M^2\right)} = 0$$

Since $0 < K < 1$, optimisation by K has no physical meaning, i.e., the power of the unit is the highest when the coefficient of electric load is at its maximum, i.e., at $K = 1$. This result is obvious since, with the specified ΔT_0, the power of the MHD generator does not depend on its operating conditions and the power required to drive the compressor is minimum at the highest possible value of the internal efficiency of the generator, i.e., at $K = 1$.

Account for the friction and heat transfer when $\Delta N_{ex} = 0$ leads us to the conclusion that the optimum value of K decreases but is always greater than 0.5.

If we disregard the heat transfer to the wall and the capacity of the compressor we can find the coefficient of electric load and the flow rate which ensure the maximum power of the MHD generator. In this case, $K_{opt} = 0.5$ and the optimum flow rate is determined from (2.16) and (2.17).

Thus, the optimum value of the coefficient of electric load, at which ΔN_u is maximum at the given ΔT_0, will be

$$1 > K_{opt} > 0.5, \tag{2.24}$$

its value being dependent on the characteristics of the magnetic system, cycle parameters and the flow of the working substance through the channel of the MHD generator.

It is difficult to determine the optimum flow rate from (2.22) analytically. However, an elementary consideration shows that at $M < 1$ the friction and heat transfer to the wall reduce the optimum value of M found from (2.16) and (2.17).

2.6. An analogous consideration of the effect produced by the operating conditions of the MHD generator on its internal efficiency

$$\eta_{oi} = \frac{\Delta N_M}{m c_p T_0 \left[1-\left(1-\frac{\Delta p_0}{p_0}\right)^{\frac{\gamma-1}{\gamma}}\right]} \tag{2.25}$$

leads us to the following conclusions;

1. If the heat transfer to the wall and the friction may be neglected K = 1 will be optimum and the flow rate will affect the internal efficiency as follows:

$$\eta_{oi} = \frac{K}{1+\frac{\gamma-1}{2}M^2(1-K)}, \tag{2.26}$$

i.e., the maximum value of the internal efficiency will be attained at $M \to 0$. This result shows that a considerable increase in M number in the channel of a MHD generator is highly undesirable from the energetic viewpoint.

2. The optimum value of K at which the internal efficiency of the generator is maximum proves greater than the value found from the condition of the maximum of the unit useful power. This is due to the fact that the internal efficiency accounts only for the dissipation of the energy as a result of friction and Joule heat, while the useful power also includes the heat transfer through the wall and the power spent to excite the field.

3.1. The optimisation of the operating conditions of the MHD generator for an elementary cycle can be extended to the unit as a whole. For this purpose let us break the entire cycle of the unit into a number of elementary cycles abcd (Fig. 1). We can assert that if each elementary cycle taken separately is optimum, then, to the first approximation, the plant as a whole will operate at the optimum duty. It should also be noted that the conclusions obtained above allow a more judicious approach to the problem of selecting the temperature at the output of the MHD generator.[x] Indeed, if we equate (2.22) to zero, we can find such value of the gas conductivity σ at which the useful power will not be generated, i.e., this condition determines the lower boundary of the expediency of utilising the magnetohydrodynamic method of energy transformation. Formula (2.22) shows that the lower boundary of conductivity, or of the temperature, drops as the gas flow is increased through the generator channel.

[x] Literary sources usually indicate that the value of the temperature at the output of the MHD generator channel is selected from the condition of sufficient gas conductivity and is specified at about 2100°C.

3.2. Even in the case of simplifying assumptions, an analytical consideration of the integral formula (1.6) encounters considerable difficulties. For this reason, the calculations were performed by numerical integration on a type M-20 computer. Below we give the results of the variational calculations of the unit with a MHD generator disregarding the power spent to excite the magnetic field.

The following parameters were assumed constant over the length of the generator channel: $\beta = 2$ Wb/m^2; $\varkappa = \frac{\delta}{n} = 0.5$; $\Delta T_w = T_0 - T_w = 500^\circ$; u; k and the coefficient of friction $\xi = 0.015$. The working substance in the channel of the MHD generator was a monoatomic gas ($\gamma = 1.67$) with the molecular weight of $\mu = 4$ ($C_p = 5{,}200$ $\frac{\text{Joule}}{\text{kg } ^\circ\text{K}}$). The number Pr = 0.681.

The heat conductivity of the gas was determined from the formula

$$\lambda_f = \lambda_0 \frac{273 + C_\lambda}{T_f + C_\lambda} \left(\frac{T_f}{273}\right)^{3/2},$$

the viscosity

$$\mu_f = \mu_0 \frac{273 + C_\mu}{T_f + C_\mu} \left(\frac{T_f}{273}\right)^{3/2}$$

where

$$\lambda_0 = 0.142 \frac{\text{Joule}}{\text{m sec } ^\circ\text{K}}$$

$$\mu_0 = 0.186 \times 10^{-4} \frac{\text{N sec}}{\text{m}^2}$$

$$C_\mu = C_\lambda = 80^\circ$$

At large values of $T_f = \frac{T_0 + T_w}{2}$ we have

$$\lambda_f = 0.0783 \sqrt{T_0 + T_w},$$

$$\mu_f = 1.03 \times 10^{-5} \sqrt{T_0 + T_w}$$

The electric conductivity of the gas was found from the formula

$$\sigma = \sigma_* \left(\frac{T}{T_*}\right)^a \sqrt{\frac{P_*}{P}}$$

where σ_* = 10 mho/m is the conductivity of the gas at T_* = 2073°K, P_* = $0.98 \times 10^5 \frac{N}{m^2}$, a = 12.

The calculations were done within a wide range of the working substance flow (m = 0.12 to 120 kg/sec), flow rates (u = 500 to 2,000 m/sec), coefficients of electric load (K = 0.3 to 0.9) and the temperature drops (T_M = $T_{o1} - T_{o2}$ = 200 to 800°) employed in the MHD generators. The principal part of the calculations was performed for T_{o1} = 2273°K and P_{o1} = $1.08 \times 10^5 \frac{N}{m^2}$. The temperature of the working substance at the compressor input was assumed equal to T_{1c} = 308 K. The efficiency of the compressor was η_c = 0.85.

3.3. Fig. 4 shows the effect produced by the flow rate on the specific power of the MHD generator $E_{ML} = \frac{N_M}{mL_g}$ at m = 0.12 kg/sec, K = 0.5. As can be seen, the maximum E_{ML} is attained at u $\simeq$ 1,100 m/sec irrespective of T_{o2}. Moreover, the optimum value of the flow rate depends neither on the coefficient of electric load nor on the flow of the working substance and is in a fairly good agreement with formula (2.16) obtained from the consideration of an elementary generator.

The effect of the flow rate on the specific take-off of the energy on the unit with MHD generator $E_{uL} = \frac{N_u}{mL_g}$ is illustrated in Fig. 5. It can be seen from the comparison with Fig. 4 that in this case the maximum is noticeably shifted towards u < 1,100 m/sec, the shift being greater at a higher temperature drop used (the smaller T_{o2} is). As K increases the value of u_{opt} is likewise displaced towards smaller flow rates. The increase in the flow rate produces a reverse effect and in the limit, when m $\simeq$ 120 kg/sec the optimum value of the flow rate approaches the value determined from (2.16).

The analogous curves plotted for specific power, as referred to the unit volume of the generator channel, are represented in Figs.6, 7 and 8. In this case the maximum value of the specific power of the MHD generator N_{Mv} (Fig. 6) is attained irrespective of T_{o2} at $u \simeq 1{,}350$ m/sec which is in good agreement with formula (2.20). When the coefficient of electric load and gas flow rate change, the value of u_{opt} remains the same. The maximum of the specific power N_{uv} (Fig. 7 and 8) is attained at slower flow rates. When the flow rate and the temperature diminish at the channel output the maximum N_{uv} shifts towards smaller flow rates. An analogous result is obtained when the coefficient of electric load is increased. Consequently, the displacement of the optimum towards smaller flow rates is due to the friction and heat transfer to the channel walls.

3.4. The effect of the coefficient of electric load on the specific power of the unit, as referred to the generator volume V_g, is illustrated in Figs.9, 10, 11 and 12. The specific power of the MHD generator N_{Mv} at $K = 0.5$ is taken as unity for all the curves. The dash lines show the curves of the change in the specific power of the generator for the case of a noncompressible fluid with a constant conductivity /1/.

It follows from the comparison of the curves that as the temperature drop increases the deviation from the "standard" (dash curve) increases too, in which case, if at $K > 0.5$ and $m = 1.2$ kg/sec (Figs 9, 10) the curves are above the "standard" curve, then at $m = 120$ kg/sec (Figs 11 and 12) they are located below. This change in $N_{\overline{Mv}} = f(k)$ owes its origin to the compression and the dependence of the gas conductivity on pressure and also to heat transfer to the wall. Indeed, if we neglect all the losses, except the Joule losses, then as K increases, at

the fixed heat value, the pressure at the generator output increases and the average gas conductivity is therefore decreased in the generator channel. This shifts the maximum $\bar{N}_{Mv}$ towards $K < 0.5$; and, when $K > 0.5$, N_{Mv} is located below the "standard" curve. This explains the deviation of the curves $\bar{N}_{Mv} = f(k)$ at m = 120 kg/sec from the "standard" curves.

At a lower gas flow rate the effect of friction increases sharply, as a result of which the change in the pressure at the generator output, depending on K, decreases as can be seen from the curves $\bar{N}_{Mv}$. For this reason, the average value of the gas conductivity at $K > 0.5$ decreases less intensively and the curve $\bar{N}_{Mv} = f(k)$ should approach the "standard" curve. However, since the generator output which operates less efficiently due to the reduced conductivity brought about by increased heat transfer to the wall becomes much shorter at small flow rates, the curve $\bar{N}_{Mv} = f(k)$ is in actual fact slightly above the "standard" curve. This can also explain the effect of the flow rate on the nature of $\bar{N}_{Mv} = f(k)$.

Figs. 9, 10, 11 and 12 also show the curves of the change in the specific power of the unit $\bar{N}_{uv}$. It can be easily seen that the optimum value of the coefficient of electric load lies in the region K = 0.6 to 0.7, changing but little in the case of a substantial alteration of the used temperature drops, flow rates and the flow of the working substance through the channel of the MHD generator. It should be pointed out, however, that as the gas flow rate decreases the maximum attainable value of $\bar{N}_{uv}$ increases somewhat and shifts towards greater K. An increase in the flow rate will reduce $\bar{N}_{uv}$ due to greater friction losses, i.e., the power required to drive the compressor.

The above thesis is clearly illustrated in Figs. 13 and 14 which show the change in the power of the MHD generator as referred to kg of gas $\bar{E}_M = \frac{N_M}{m}$ and the unit as a whole $\bar{E}_{sp}$. The calculations show that the curve K = 0.5 at m = 120 kg/sec (Fig. 13) practically coincides with the theoretical curve for the case involving no heat transfer to the channel wall, i.e., in this case the relative share of heat losses is negligibly small. As the coefficient of electric load increases and the gas flow rate diminishes the value of $\bar{E}_M$ decreases in which case the greatest deviation of the curves from the linear law $\Delta \bar{E}_M = C_p \Delta T_0$ is observed in the region of the smaller temperatures, which can be explained by an increase in the relative share of heat transfer through the walls. It is interesting to note that at the small flow of the working substance the decrease in T_{02} (increased temperature drop in the generator) below a definite value does not increase the MHD generator power. Hence, when the power of the MHD generators is small it is irrational to increase the used heat content.

We cannot but fail to notice the fact that the referred power of the unit $\bar{E}_{sp}$ (Fig. 14) at $m > 12$ kg/sec is greater at $K \simeq 0.7$ to 0.9, whereas at $m < 12$ kg/sec the maximum is attained at K = 0.5. This can be explained by the fact that at $m < 12$ kg/sec the predominant role is played by the dissipation friction losses and the heat transfer to the wall, whereas at $m > 12$ kg/sec the main losses are due to the dissipation of the Joule heat. Therefore, an increase in K essentially reduces the relative consumption of the power produced by the MHD generator to drive the compressor. It should be noted in conclusion that at small flow rates we observe an insufficiently expressed maximum of the referred power of the unit $\bar{E}_{sp}$.

3.5. The effect of the flow rate, the coefficient of electric load and the gas temperature at the generator channel output on the internal efficiency η_{oi} of the energy transformation process is shown in Figs 15 and 16. It can be seen that as K increases and the flow rate of the working substance and the temperature at the output T_{o2} decrease, the effect of the flow rate on η_{oi} increases noticeably, which can be attributed to the greater role played by the dissipation heat losses. It should be noted that if at K = 0.5 an increase in the used temperature drop (decrease of T_{o2}) somewhat increases η_{oi} then, at K = 0.9, we observe the decrease in η_{oi} in which case, as the flow rate increases and T_{o2} diminishes, the curves $\eta_{oi} = f(T_{o2})$ for K = 0.5 and K = 0.9 draw near to each other, especially when m = 12 kg/sec.

Fig. 17 shows the change in the internal efficiency of the MHD generator depending on K. The figure shows that there is an optimum value of K at which η_{oi} is at its maximum, the optimum K shifting towards the smaller values with the decrease in the gas flow and the increase in the flow rate. Analogous curves for the specific power of the unit $\bar{E}_{sp} = \frac{N_u}{m}$ are given in Fig. 18, where $\bar{E}_{sp}$ increases essentially at a higher gas flow. The optimum value of K increases with the increase in m. The presence of the maximum η_{oi} and $\bar{E}_{sp}$ is due to the effect produced by friction and heat transfer to the wall. Indeed, as K increases, the length of the generator becomes much longer and, with $K \longrightarrow 1$, the length of the generator in the absence of heat transfer to the wall grows infinitely large, i.e., the friction losses increase intensively.

In Fig. 18 the dotted lines show, by way of comparison, the change in the internal efficiency. It follows from this that the maximum $\bar{E}_{sp}$ can be attained at smaller

values of K. As has been shown above, this can be attributed to the fact that the internal efficiency accounts only for the dissipation losses, whereas the useful power of the unit is also determined by the heat transfer to the walls of the generator channel. If we also take into account the power spent to excite the field, the maximum $\bar{E}_{sp}$ will be displaced still more towards the smaller values of the coefficient of electric load.

This results shows beyond all doubt that the role of the internal efficiency of the process, as a criteria of the efficiency of the unit as a whole, is considerably reduced in magnetohydrodynamic units and the value of the useful power of the unit, as referred to the flow of the working substance, becomes the principal factor. Herein lies the main difficulty of optimisation of the parameters of the unit with a MHD generator.

References

1. J.Neuringer, J.Fluid Mech. 7, pt 2, 1960.
2. Energy Conversion for Space Power. Academic Press, New-York, London 1961.
3. N.I.Polsky, G.M.Shchegolev. Thermal Physics of High Temperatures, No. 1, 1964.
4. N.I.Polsky, Thermal Physics of High Temperatures, No. 2. 1964.
5. R.J.Rosa. Phys. Fluids, 4, No. 2, 1961.
6. A.E.Sheindlin, A.B.Gubarev, V.I.Kovbasyuk, V.A.Prokudin. Proceedings of the USSR Academy of Sciences, Energetics and Automatics, No. 6, 1962.

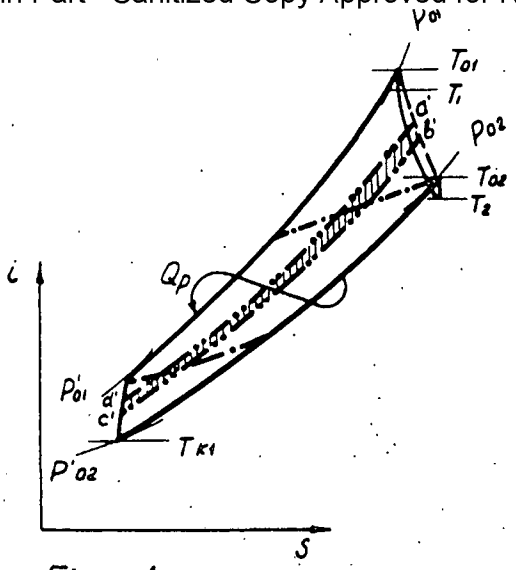

Fig : 1

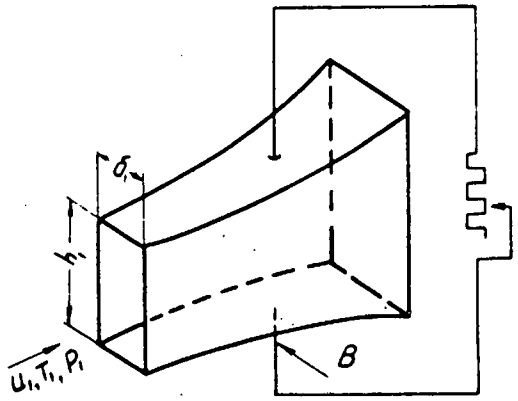

Fig : 2

Fig : 3

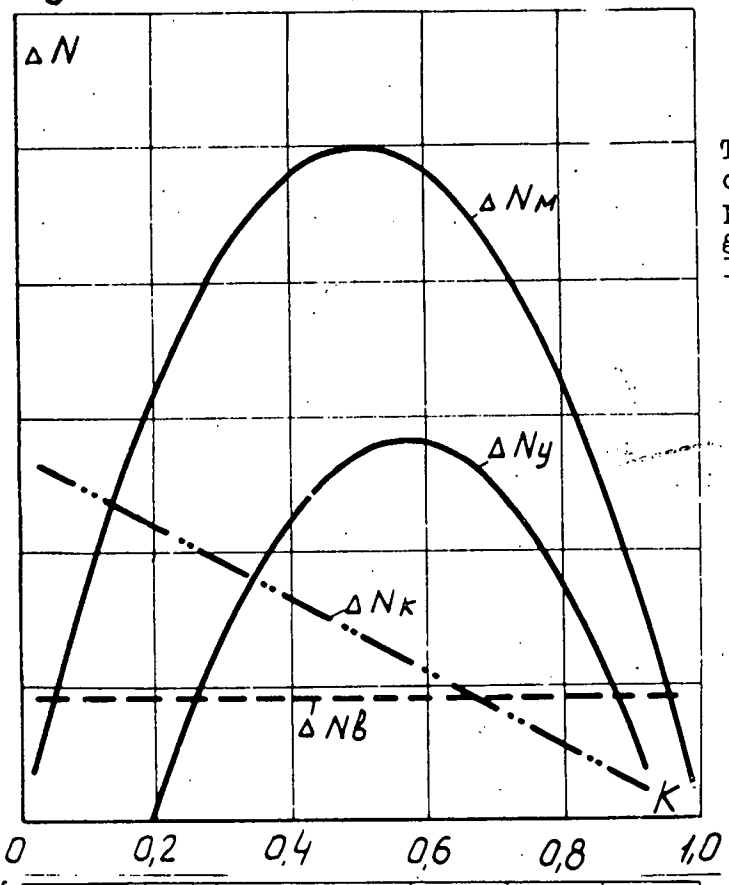

The effect of the coefficient of electric load on the useful power of the unit with an MHD generator with a specified length of the channel.

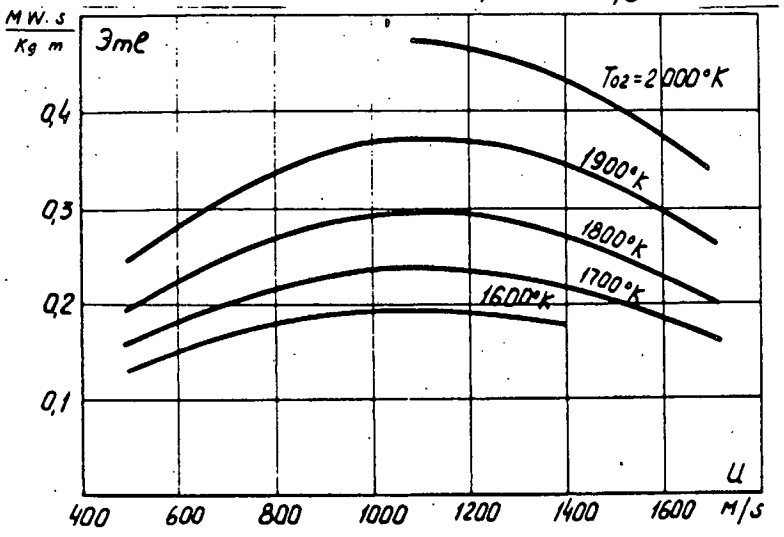

Fig : 4

The effect of the flow rate on the specific power of an MHD generator $E_{ML} \frac{N_M}{m L_g}$

(T_{01} = 2273°K, P_{01} = 1.1 ata, m = 0.12 kg/sec, K = 0.5)

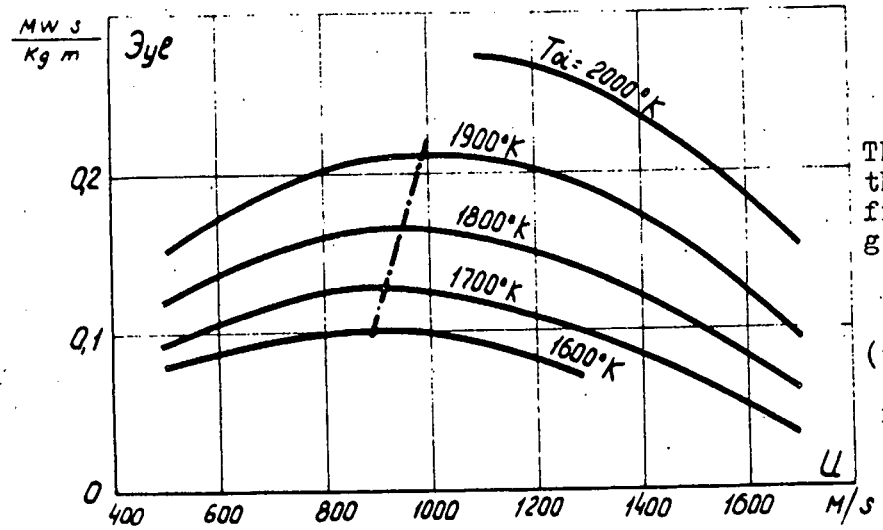

Fig: 5

The effect of the flow rate on the specific take-off of energy from the unit with an MHD generator $E_{uL} = \frac{N_u}{m L_g}$

($T_{01} = 2273^{\circ}K$, $P_{01} = 1.1$ ata, $m = 0.12$ kg/sec, $K = 0.5$)

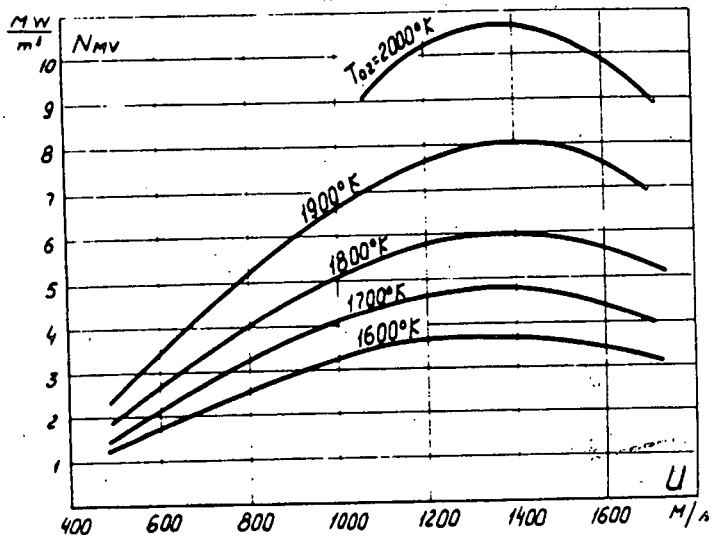

Fig: 6

The effect of the flow rate on the specific power of an MHD generator $N_{MV} = \frac{N_M}{V_g}$

($T_{01} = 2273^{\circ}K$, $P_{01} = 1.1$ ata, $m = 0.12$ kg/sec, $K = 0.5$)

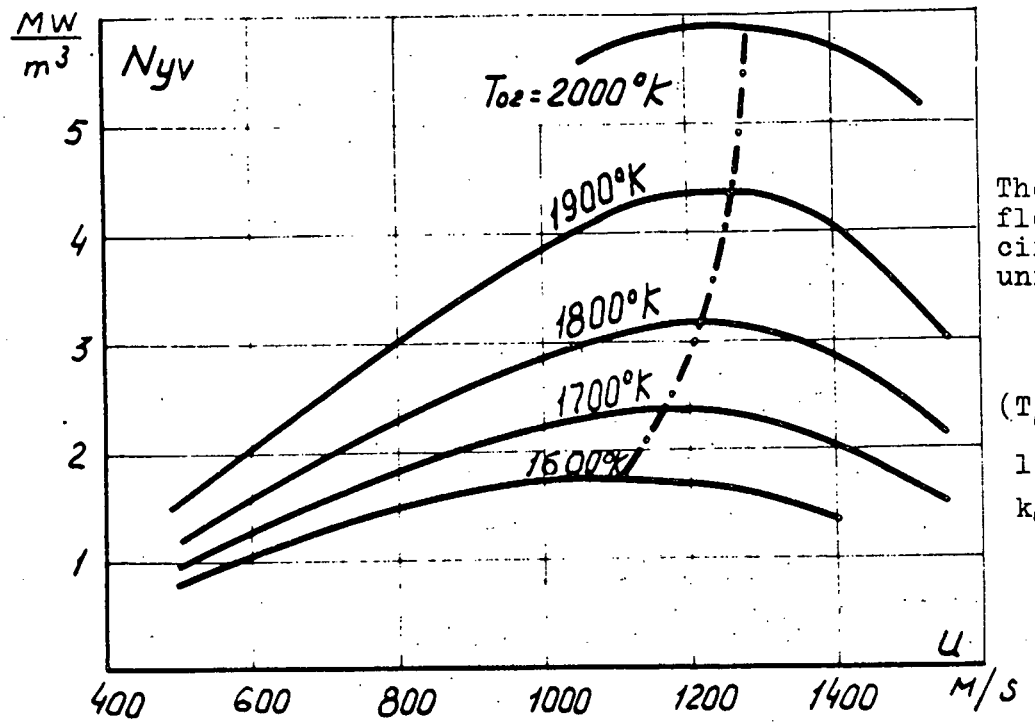

Fig: 7

The effect of the flow rate on the specific power of the unit $N_{uv} = \frac{N_u}{V_g}$

($T_{01} = 2273^{\circ}K$, $P_{01} = 1.1$ ata, $m = 0.12$ kg/sec, $K = 0.5$)

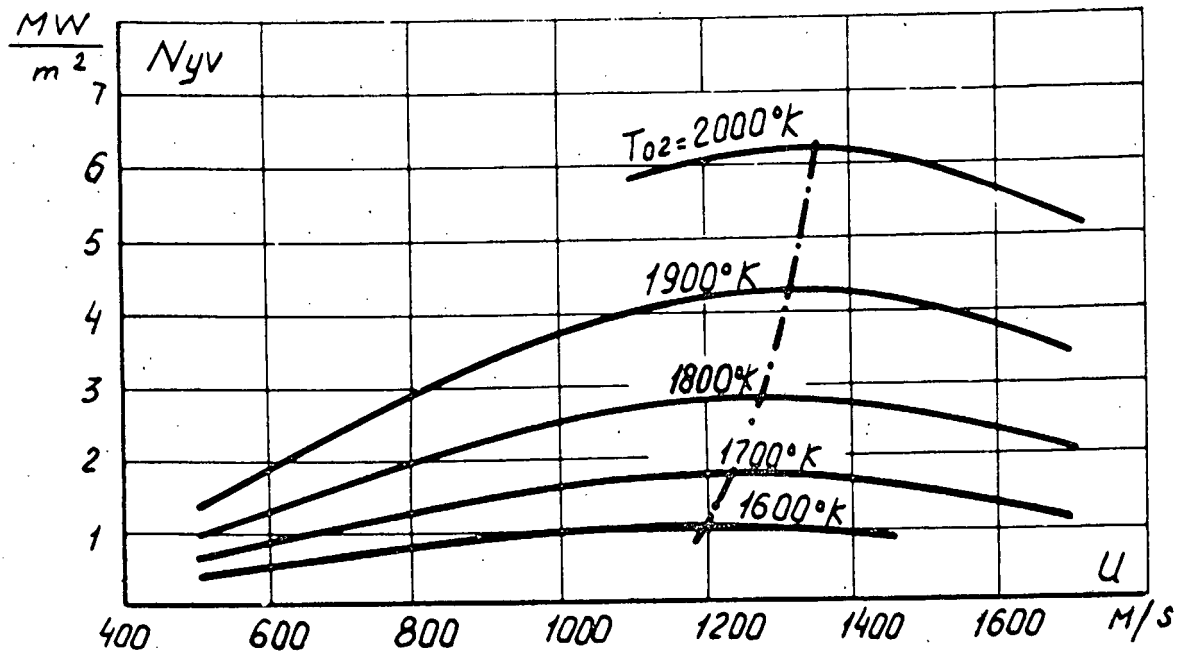

Fig : 8

The effect of the flow rate on the specific power of the unit $\bar{N}_{uv} = \frac{N_u}{V_g}$

(T_{01} = 2273°K, P_{01} = 1.1 ata, m = 120 kg/sec, K = 0.5).

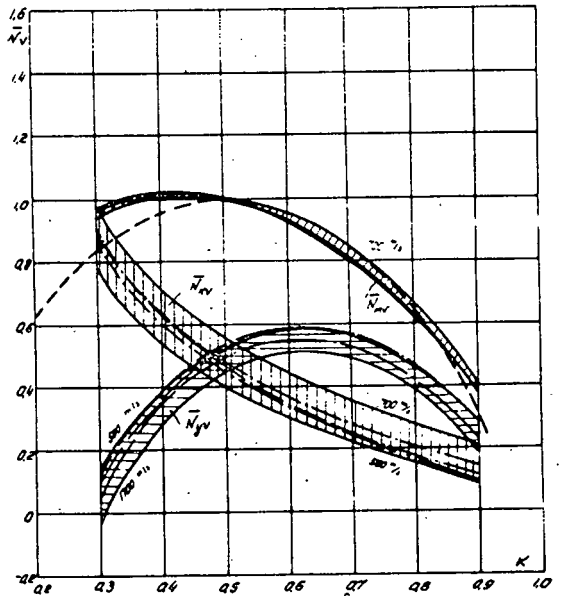

Fig : 9

The effect of the coefficient of electric load on the specific power of the unit $\bar{N}_v$

(T_{01} = 2273°K, T_{02} = 1800°K, P_{01} = 1.1 ata, m = 1.2 kg/sec)

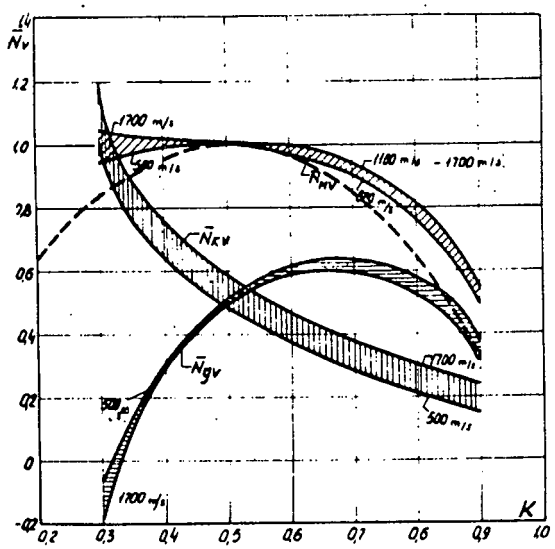

Fig : 10

The effect of the coefficient of electric load on the specific power of the unit $\bar{N}_v$

(T_{01} = 2273°K, T_{02} = 1600°K, P_{01} = 1.1 ata, m = 1.2 kg/sec)

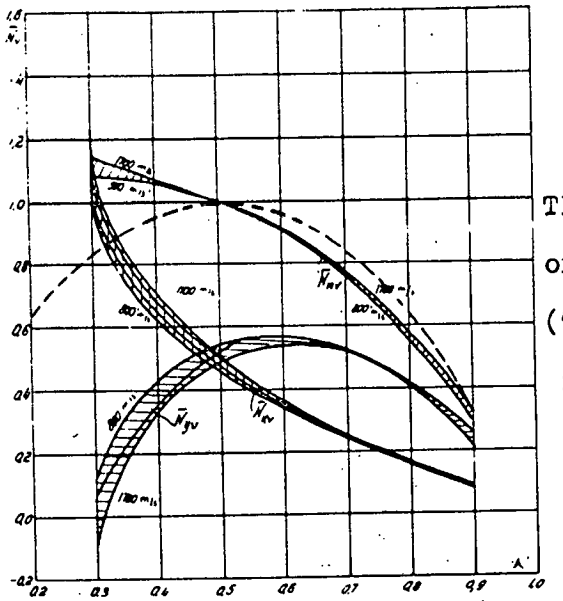

Fig: 11

The effect of the coefficient of electric load on the specific power of the unit $\bar{N}_v$ ($T_{o1} = 2273^oK$, $T_{o2} = 1800^oK$, $P_{o1} = 1.1$ ata, $m = 120$ kg/sec).

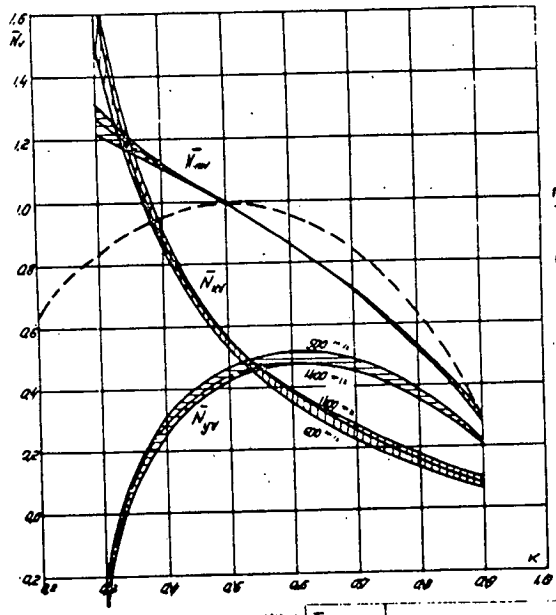

Fig: 12

The effect of the coefficient of electric load on the specific power of the unit $\bar{N}_v$ ($T_{o1} = 2273^oK$, $T_{o2} = 1600^oK$, $P_{o1} = 1.1$ ata, $m = 120$ kg/sec).

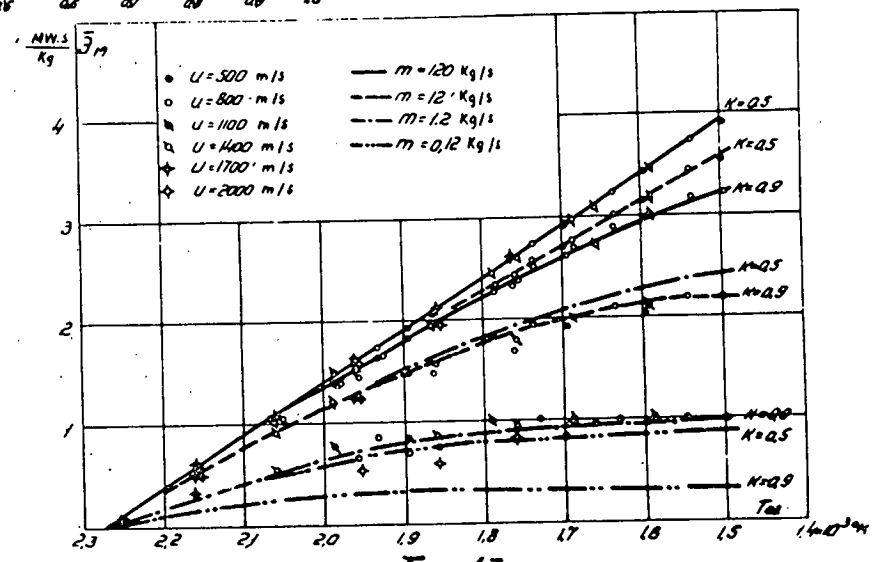

Fig: 13

The effect of T_{o2} and the gas flow on the referred power of a MHD generator $\bar{E}_M = \frac{N_M}{m}$ (m = 2273°K, P_{o1} = 1.1 ata).

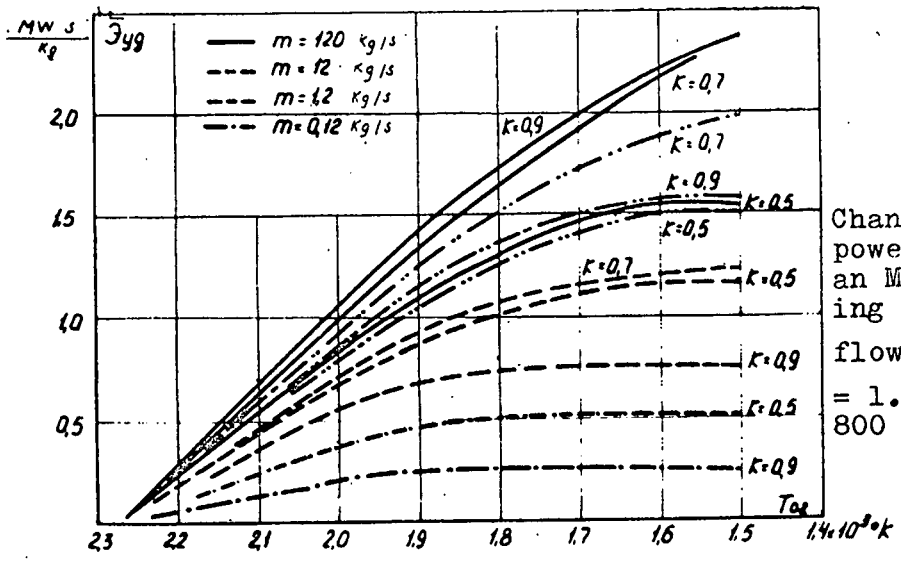

Fig: 14

Change in the referred power in the unit with an MHD generator depending on T_{02} and the gas flow (T_{01} = 2273°K, P_{01} = 1.1 ata, u = 500 to 800 m/sec)

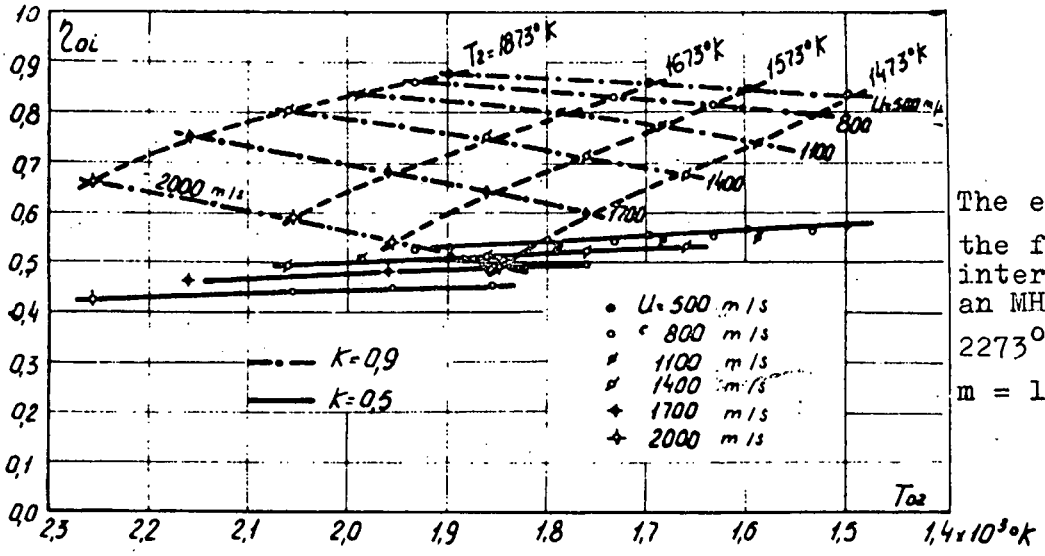

Fig: 15

The effect of T_{02} and the flow rate on the internal efficiency of an MHD generator (T_{01} = 2273°K, P_{01} = 1.1 ata, m = 12 kg/sec)

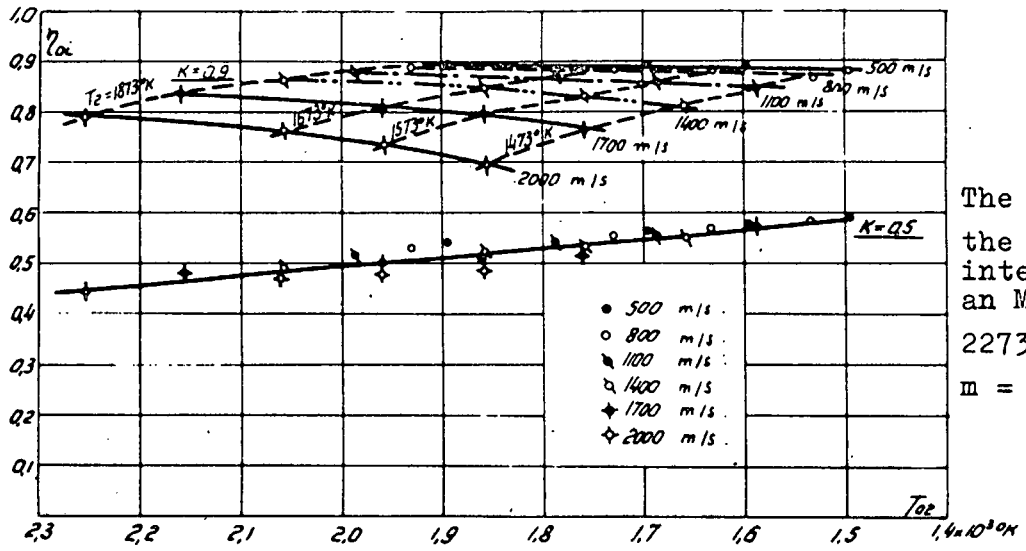

Fig: 16

The effect of T_{02} and the flow rate on the internal efficiency of an MHD generator (T_{01} = 2273°K, P_{01} = 1.1 ata, m = 120 kg/sec)

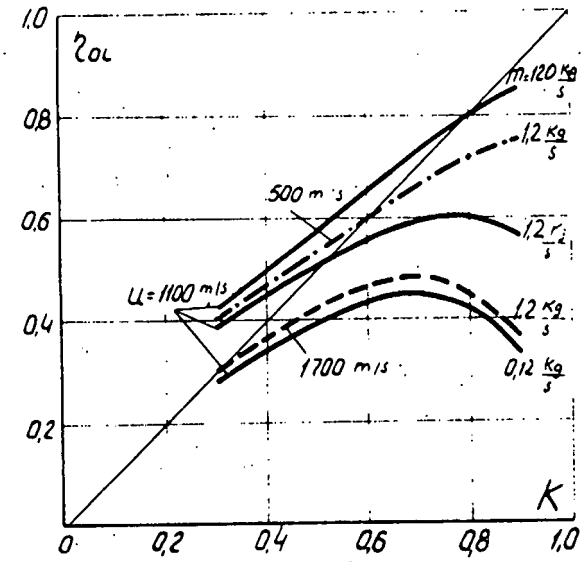

Fig: 17

The effect of the coefficient of electric load on the internal efficiency of MHD generator (T_{o1} = 2273°K, P_{o1} = 1.1 ata, T_2 = 1473°K).

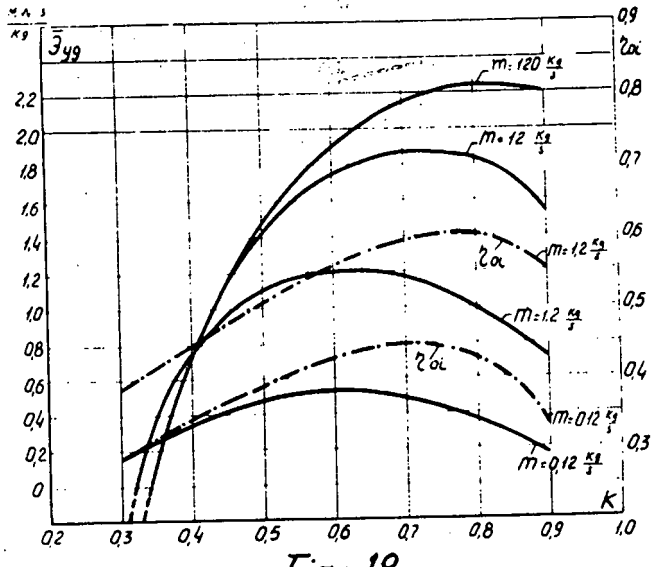

Fig: 18

The effect of the coefficient of electric load on the referred power of the unit with MHD generator $\bar{E}_{sp} = \frac{N_u}{m}$ (T_{o1} = 2273°K, T_{o2} = 1590°K, P_{o1} = 1.1 ata, u = 1,100 kg/sec).